Bioorganic Chemistry 92 (2019) 103273

Contents lists available at ScienceDirect

Bioorganic Chemistry

journal homepage: www.elsevier.com/locate/bioorg

Discovery of 2-ethoxy-4-(methoxymethyl)benzamide derivatives as potent and selective PTP1B inhibitors

Fangzhou Xie[a], Yaoyao Liang[a], Yu Xia[a,b], Shuhua Luo[a], Faqin Jiang[a], Lei Fu[a,*]

[a] Shanghai Key Laboratory for Molecular Engineering of Chiral Drugs, School of Pharmacy, Shanghai Jiao Tong University (SJTU), 800 Dongchuan Road, Shanghai 200240, China

[b] Viva Biotech (Shanghai) Limited, Shanghai 201203, China

ARTICLE INFO

Keywords:
PTP1B Inhibitors
Selectivity
2-Ethoxy-4-(methoxymethyl)benzamide
Type 2 diabetes

ABSTRACT

Protein tyrosine phosphatase 1B (PTP1B), a key negative regulator of insulin signaling, is considered as a promising and validated therapeutic target for type 2 diabetes mellitus (T2DM) and obesity. Upon careful study, a series of 2-ethoxy-4-(methoxymethyl)benzamide and 2-ethoxy-5-(methoxymethyl)benzamide analogs designed by the "bioisosteric principle" were discovered, wherein their PTP1B inhibitory potency, type of PTP1B inhibition, selectivity and membrane permeability were evaluated. Among them, compound **10m** exhibited high inhibitory activity (IC_{50} = 0.07 μM), significant selectivity (32-fold) over T-cell PTPase (TCPTP) as well as good membrane permeability (P_{app} = 2.41 × 10^{-6} cm/s). Further studies on cell viability and cellular activity revealed that compound **10m** could enhance insulin-stimulated glucose uptake with no significant cytotoxicity.

1. Introduction

Protein tyrosine phosphatase 1B (PTP1B) is the first isolated enzyme from the protein tyrosine phosphatases (PTPs) family, and played an important role in both the insulin and leptin signaling pathways [1–3]. As a key member of the PTPs family, PTP1B maintains proper levels of tyrosine phosphorylation and regulate cellular processes including growth, differentiation, metabolism, migration and survival [4–7], thereby modulate glucose and lipid metabolism [8]. An overexpression of PTP1B causes persistent dephosphorylation of the insulin receptor (IR), eventually leading to insulin resistance and type 2 diabetes [9]. Research in PTP1B knockout rodents has revealed that the lack of PTP1B gene resulted in an improved insulin sensitivity and resistance to diet-induced obesity without affecting normal growth and longevity. This has indicated that PTP1B is a promising drug target for the treatment of type 2 diabetes and obesity [10–12].

Within the last decade, various PTP1B inhibitors have been discovered [9,13,14]. Meanwhile, only a few of these compounds can enter clinical research [15]. The major challenges of previously developed PTP1B inhibitors include weak selectivity and poor cell-permeability [16,17]. Weak selectivity of PTP1B inhibitors is a consequence due to the high sequence homology of the active site within PTPs family, especially PTP1B and T-cell protein tyrosine phosphatase (TCPTP), while poor cell-permeability is resulted from high ionization of the inhibitors in a physiological situation [18–20]. Therefore, improvements of molecular selectivity and membrane permeability are the new trends for research on PTP1B inhibitors [21,22].

As of recently, our laboratory has reported the discovery of various lead compounds (Fig. 1, compounds **I–III**) which are a novel class of PTP1B inhibitors [23,24]. Among such, the Y-shaped bisarylethenesulfonic acid esters (compound **III**) can interact with the catalytic site (A site) and multiple secondary binding sites (C and E site) of PTP1B, displaying high potency, good membrane permeability, and acceptable PTP1B selectivity [25].

We sought to improve the potency and selectivity of lead compound **III**, so we replaced one of the arylethenesulfonic acid ester groups in compound **III** with salicylic acid moiety. Within medical chemistry, bioisosteric replacement is one of the most efficient approaches for modifying and improving the properties of a lead compound such as selectivity and potency [26]. Additionally, due to previous efforts on the pTyr binding site (catalytic site) of PTP1B, salicylic acid group was discovered as an excellently potent pTyr mimetic with cell-permeability [27–30]. As a result, this bioisosteric replacement was expected to improve the potency and selectivity of compound **III** while retaining its cell-permeability.

We designed, synthesized and evaluated a series of 2-ethoxy-4-(methoxymethyl)benzamide and 2-ethoxy-5-(methoxymethyl)benzamide derivatives in order to further explore the structure–activity relationships and search for improved PTP1B inhibitors. When one arylethenesulfonic acid ester group was replaced by salicylic acid moiety,

* Corresponding author.
E-mail address: leifu@sjtu.edu.cn (L. Fu).

https://doi.org/10.1016/j.bioorg.2019.103273
Received 26 June 2019; Received in revised form 14 August 2019; Accepted 9 September 2019
Available online 10 September 2019

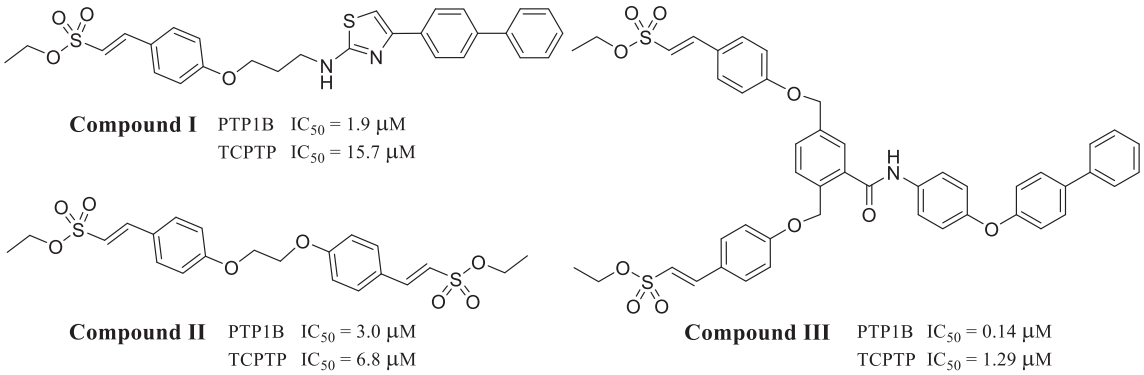

Fig. 1. Representative arylethenesulfonicacid ester PTP1B inhibitors.

some of these derivatives exhibited better PTP1B inhibitory activity and selectivity than lead compound **III**. As the most potent and selective PTP1B inhibitor in this study, compound **10m** could enhance insulin-stimulated glucose uptake with no significant cytotoxicity. This research provides great insight and valuable information on further discovery of novel PTP1B inhibitors with higher potency and better selectivity.

2. Result and discussion

2.1. Chemistry

The designed compounds **6a-6c** and **10a-10p** were synthesized according to the method outlined in Scheme 1**.** The synthesis began with the commercially available 2-hydroxy-4-methylbenzoic acid to afford the requisite intermediate **5** or **9** through a long synthetic sequence, which included esterification, bromination, twice substitution, Wittig-Horner reaction [24] and hydrolysis in sequence. After condensation with various amines and deprotection, intermediate **5** or **9** was converted to the target compounds **6a-6c** and **10a-10p** respectively.

The preparation of the designed compounds **16a-16c** and **20a-20c** required a long synthetic sequence as well (Scheme 2). First, intermediate **13** and **17** were synthesized from tert-butyl 5-formyl-2-hydroxybenzoate by reduction, protection, substitution and deprotection. Through the Mitsunobu reaction, Wittig-Horner reaction and hydrolysis, intermediate **13** or **17** was subsequently converted to intermediate **15** or **19** respectively. Then, intermediate **15** or **19** underwent the same reaction as intermediate **5** or **9** in Scheme 1 to provide target compounds **16a-16c** and **20a-20c** respectively.

2.2. PTP1B inhibitory activity and structure-activity relationship

In order to replace one of the arylethenesulfonic acid ester groups by salicylic acid moiety and discover potent, selective and cell-

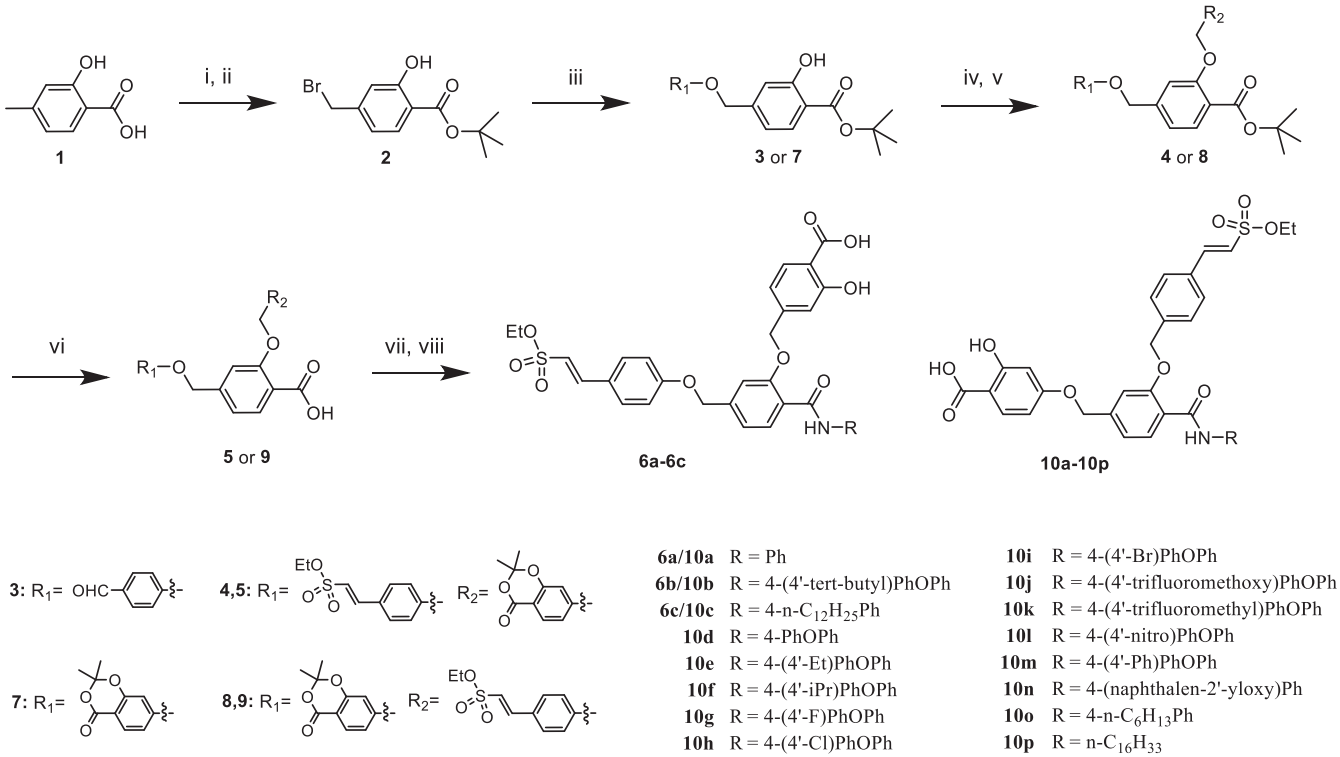

6a/10a	R = Ph
6b/10b	R = 4-(4'-tert-butyl)PhOPh
6c/10c	R = 4-n-$C_{12}H_{25}$Ph
10d	R = 4-PhOPh
10e	R = 4-(4'-Et)PhOPh
10f	R = 4-(4'-iPr)PhOPh
10g	R = 4-(4'-F)PhOPh
10h	R = 4-(4'-Cl)PhOPh
10i	R = 4-(4'-Br)PhOPh
10j	R = 4-(4'-trifluoromethoxy)PhOPh
10k	R = 4-(4'-trifluoromethyl)PhOPh
10l	R = 4-(4'-nitro)PhOPh
10m	R = 4-(4'-Ph)PhOPh
10n	R = 4-(naphthalen-2'-yloxy)Ph
10o	R = 4-n-C_6H_{13}Ph
10p	R = n-$C_{16}H_{33}$

Scheme 1. Synthesis of 2-ethoxy-4-(methoxymethyl)benzamide derivatives. Reagents and conditions: (i) CDI, *t*-BuOH, DBU, rt, 5 h; (ii) NBS, AIBN, CCl_4, reflux, 4 h; (iii) *p*-hydroxybenzaldehyde or 7-hydroxy-2,2-dimethyl-4H-benzo[d][1,3]dioxin-4-one, K_2CO_3, ACN, reflux, 8 h; (iv) 7-(bromomethyl)-2,2-dimethyl-4H-benzo[d][1,3]dioxin-4-one or 4-(bromomethyl) benzaldehyde, K_2CO_3, ACN, reflux, 8 h; (v) ethyl (diethoxyphosphoryl)methanesulfonate, NaH, THF, 0 °C-rt, 6 h; (vi) TFA, DCM, rt, 1 h; (vii) amine, HATU, DIEA, DMF, rt, 1–2 h; (viii) *conc.* HCl, 1,4-dioxane, rt, 48–96 h.

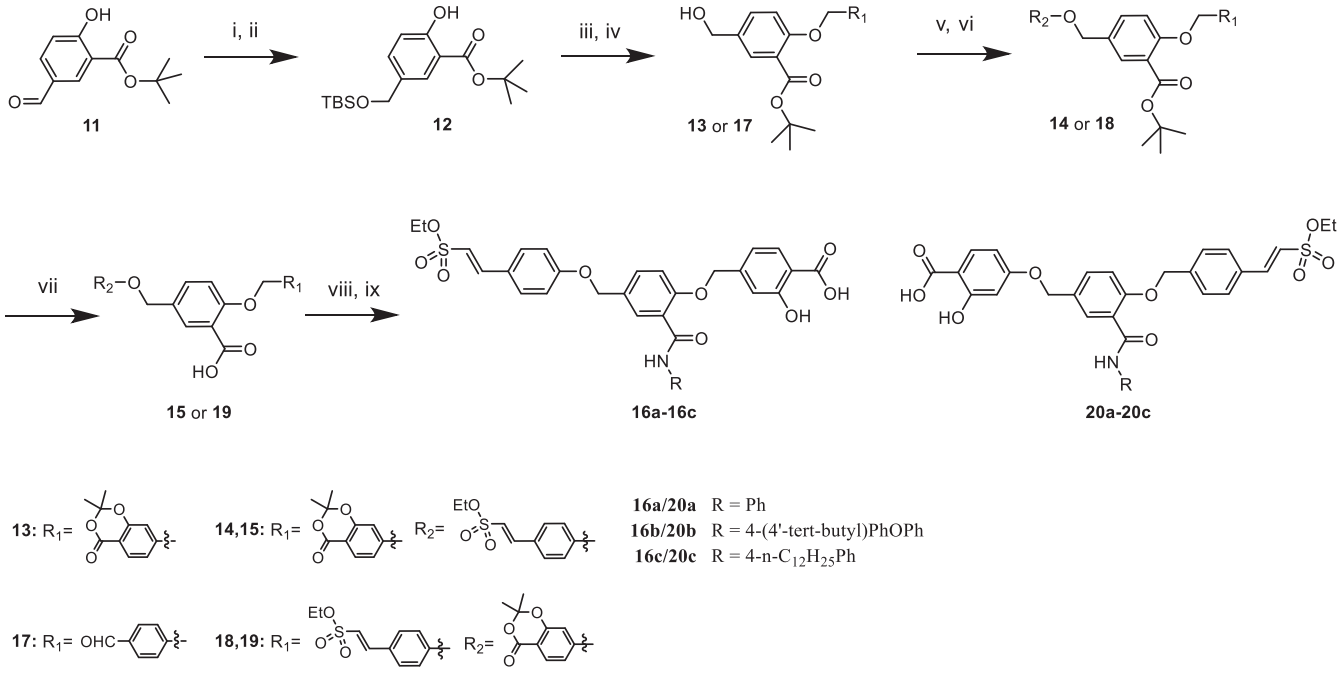

Scheme 2. Synthesis of 2-ethoxy-5-(methoxymethyl)benzamide derivatives. Reagents and conditions: (i) $NaBH_4$, MeOH, rt, 0.5 h; (ii) TBSCl, iminazole, 0 °C-rt, 12 h; (iii) 7-(bromomethyl)-2,2-dimethyl-4H-benzo[d][1,3]dioxin-4-one or 4-(bromomethyl) benzaldehyde, K_2CO_3, ACN, reflux, 8 h; (iv) TBAF, THF, rt, 1 h; (v) *p*-hydroxybenzaldehyde or 7-hydroxy-2,2-dimethyl-4H-benzo[d][1,3]dioxin-4-one, DIAD, PPh_3, THF, rt, 12 h; (vi) ethyl (diethoxyphosphoryl)methanesulfonate, NaH, THF, 0 °C-rt, 6 h; (vii) TFA, DCM, rt, 1 h; (viii) amine, HATU, DIEA, DMF, rt, 1–2 h; (ix) *conc.* HCl, 1,4-dioxane, rt, 48–96 h.

Table 1
Inhibitory activity of compounds **6a-c**, **10a-c**, **16a-c** and **20a-c** against PTP1B.[a]

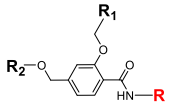

6a-c and **10a-c**

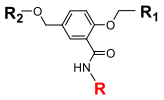

16a-c and **20a-c**

R	Compound, IC_{50}(μM)			
	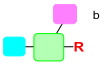	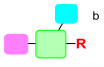	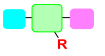	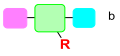
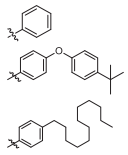	**6a**, 13.1 ± 1.7	**10a**, 1.7 ± 0.3	**16a**, 9.6 ± 1.1	**20a**, 2.1 ± 0.3
	6b, 5.4 ± 0.8	**10b**, 0.14 ± 0.03	**16b**, 3.9 ± 0.4	**20b**, 0.67 ± 0.11
	6c, 6.8 ± 0.6	**10c**, 0.47 ± 0.08	**16c**, 5.8 ± 0.7	**20c**, 0.85 ± 0.05

[b] represents the core scaffold, represents arylethenesulfonic acid ester group, represents salicylic acid group.
[a] IC_{50} values were determined by regression analysis and expressed as means ± SD of three replications.

permeable PTP1B inhibitors, we applied 2-ethoxy-4-(methoxymethyl) benzamide as well as 2-ethoxy-5-(methoxymethyl)benzamide as the core scaffolds. As shown in Table 1, compounds **6a-c** and **16a-c** showed low inhibitory activity (IC_{50} = 3.9–13.1 μM) when one salicylic acid group was introduced to R_1 (R_2 was arylethenesulfonic acid ester group). Excitingly, compared to compounds **6a-c** and **16a-c**, the introduction of one salicylic acid group to R_2 (R_1 was arylethenesulfonic acid ester group) in compounds **10a-c** and **20a-c** led to a significant increase of the inhibitory potency (e.g. compound **10b** IC_{50} = 0.14 μM, better than lead compound **III**). This result indicated that the introduction of salicylic acid group to R_2 could provide stronger interactions with PTP1B as compared to the lead compound **III**. In addition, compound **10a** (IC_{50} = 1.7 μM) showcased more potent PTP1B inhibitory activity than compound **20a** (IC_{50} = 2.1 μM), and similar phenomena were also observed in compound group **10b**/**20b** and **10c**/**20c**. This suggests that 2-ethoxy-4-(methoxymethyl)benzamide is an active core-scaffold for high PTP1B inhibitory activity. Therefore, both the position of salicylic acid moiety and the structure of core scaffold within these compounds influenced the PTP1B inhibitory activity.

Encouraged by the above findings, more 2-ethoxy-4-(methoxymethyl)benzamide derivatives (**10d-10p**) were subsequently designed and synthesized. As shown in Table 2, all of these compounds showcased potential PTP1B inhibitory activity. In addition, compounds with bigger or longer hydrophobic chains exhibited more potent PTP1B inhibitory activity (e.g., the IC_{50}s of compound **10a**/**10d**/**10m** and **10o**/**10c** followed the sequences of **10a** > **10d** > **10m** and **10o** > **10c**), demonstrating that bigger or longer hydrophobic chains can generate increased hydrophobic interactions with PTP1B. Within the biggest hydrophobic group of this research, biphenylyloxyphenyl derivatives (**10m**, IC_{50} = 0.07 μM) were 2-fold more potent than the lead

Table 2
Inhibitory activity of compounds **10d-p** against PTP1B [a,b].

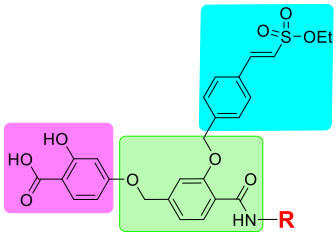

Cmpds	R	IC_{50}(μM)	Cmpds	R	Cmpds
10d	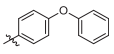	0.39 ± 0.02	**10k**	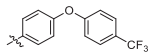	0.53 ± 0.04
10e	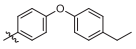	0.25 ± 0.03	**10l**	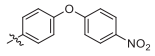	0.85 ± 0.04
10f	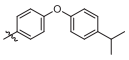	0.17 ± 0.03	**10m**	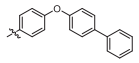	0.07 ± 0.01
10 g	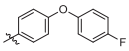	0.44 ± 0.07	**10n**	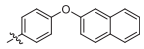	0.11 ± 0.02
10 h	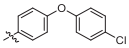	0.52 ± 0.06	**10o**	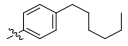	1.3 ± 0.1
10i	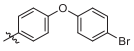	0.49 ± 0.04	**10p**	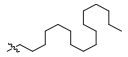	0.67 ± 0.05
10j	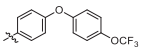	0.61 ± 0.07			

[a] IC_{50} values were determined by regression analysis and expressed as means ± SD of three replications
[b] Inhibitory activity of compounds **10a-c** is shown in Table 1.

compound **III**, indicating that 2-ethoxy-4-(methoxymethyl)benzamide derivatives have great potential of discovering potent PTP1B inhibitors.

2.3. The type of PTP1B inhibition

We selected four representative compounds (**10b**, **10f**, **10m** and **10n**) to perform enzyme kinetic experiment based on Lineweaver-Burk plot, in order to further study the mechanism of action (MOA) of these analogs,. As shown in Fig. 2(a)–(d), the straight lines in each plot had the same y intercepts, but different slopes and x-intercepts during data sets. This indicated that the Michaelis-Menten constant (K_m) was increasing while the maximum velocity (V_{max}) remained unaffected by the compound concentration. Therefore, compounds **10b**, **10f**, **10m** and **10n** were competitive inhibitors with respect to the substrates. The K_i values of compound **10b**, **10f**, **10m** and **10n** were calculated as 36 nmol/L, 84 nmol/L, 82 nmol/L and 49 nmol/L, respectively.

2.4. Selectivity over TCPTP and membrane permeability

Subsequently, the potent active compounds of IC_{50} below 0.2 μM against PTP1B (i.e. compound **10b**, **10f**, **10m** and **10n**) were further evaluated for their inhibitory activities against TCPTP. As shown in Table 3, all of these molecules showcased better selective inhibitory activity for PTP1B over TCPTP than lead compound **III**. Specifically, compound **10b**, **10f**, **10m** and **10n** showed 11–32 folds of selectivity for PTP1B over TCPTP. Among them, compound **10m** exhibited about a 4-fold increase of selectivity as compared to lead compound **III** for PTP1B over TCPTP.

In addition, the membrane permeability of these compounds were evaluated in a parallel artificial membrane permeability assay (PAMPA) [31,32]. The permeability rates (P_{app}) of these compounds (**10b**, **10f**, **10m** and **10n**) were listed in Table 3. All tested compounds showed sufficient membrane permeability (P_{app} = 1.92 to 2.41 × 10^{-6} cm/s, better than atenolol), indicating that these 2-ethoxy-4-(methoxymethyl) benzamide derivatives contain sufficient membrane permeability.

2.5. Molecular docking

We performed the molecular docking for compound **10m**, in order to understand the binding mode of 2-ethoxy-4-(methoxymethyl)benzamide analogues, and explain the high PTP1B activity as well as selectivity of these compounds. As illustrated in Fig. 3, the salicylic acid group stretches deep into the catalytic site of PTP1B, forming multiple interactions. It is a dense network of hydrogen bonds (with K121, E116 and R222) and π-π stacking reactions (with F183). In addition, the sulfonic acid ester chain forms two hydrogen bonds with Q22, while the hydrophobic chain generates multiple hydrophobic interactions (with D30, P32, C33 and k37) and hydrogen bonds (with Q263). These multiple interactions contribute to the improvements of PTP1B inhibitory activity and selectivity for 2-ethoxy-4-(methoxymethyl)benzamide analogues.

2.6. Effects of compound *10m* and *10n* on cell viability

In order to determine the cytotoxicity of 2-ethoxy-4-(methoxymethyl)benzamide derivatives, two compounds (**10m** and **10n**) were selected to evaluate their effects on HepG2 and HL-7702 cell viability by means of CCK8 assay. As shown in Fig. 4, both of the two compounds showed no cytotoxicity on HepG2 cells below 6.25 μM. From 6.25 μM to 100 μM, inhibitory effects on HepG2 cells were observed in a dose dependent manner; whereas the cytotoxicity of compounds **10m** and **10n** remained less than 37% and 32% respectively (even at 100 μM). In addition, both of the two tested compounds (**10m** and **10n**) displayed low cytotoxicity against HL-7702 cells at 100 μM (e.g. 43% and 40% cell viabilities were inhibited respectively at 100 μM). These results indicated that the newly discovered PTP1B inhibitors have no significant cytotoxicity.

2.7. Effects of compound *10m* on insulin-stimulated glucose uptake

It has been suggested that PTP1B inhibition results in a marked improvement for insulin sensitivity and glucose metabolism [33]. In

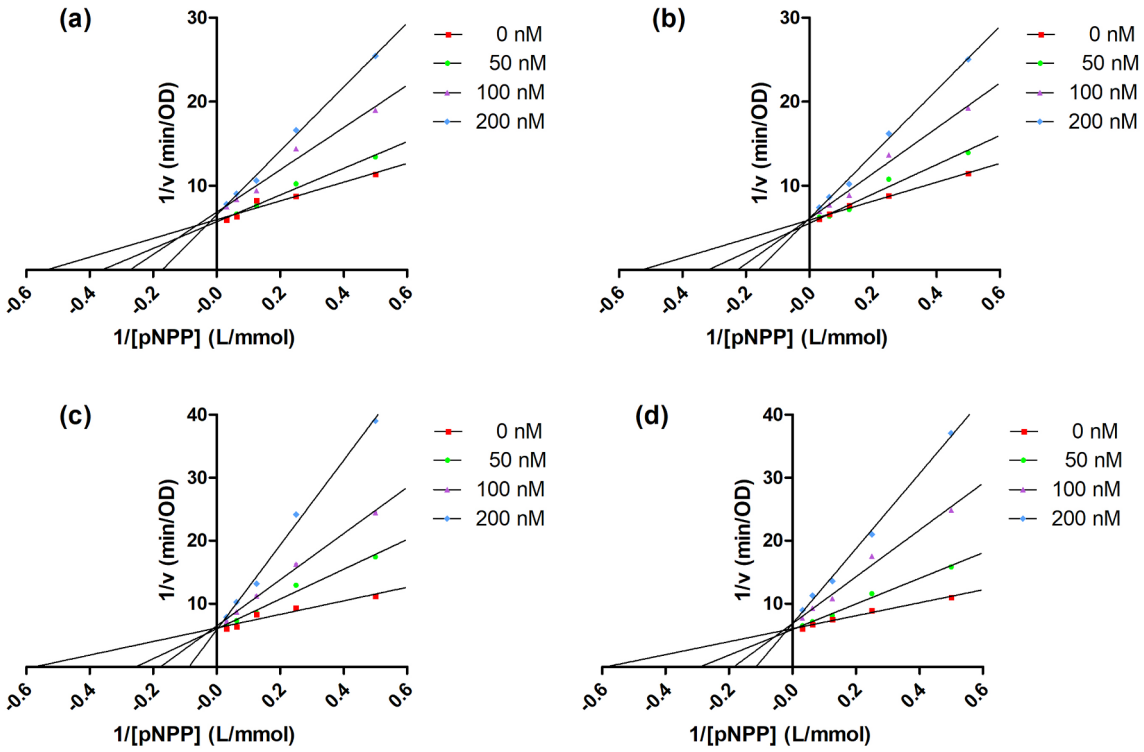

Fig. 2. (a) The Lineweaver-Burk plot of compound **10b**; (b) The Lineweaver-Burk plot of compound **10f**; (c) The Lineweaver-Burk plot of compound **10m**; (d) The Lineweaver-Burk plot of compound **10n**. In the presence of compound **10b**, **10f**, **10m** and **10n** at the concentration of 0 nM (1% DMSO, squares), 50 nM (circles), 100 nM (triangles) or 200 nM (rhombus), the reciprocal of reaction velocity (1/v) was plotted against the reciprocal of pNPP concentration ((1/[pNPP]). The values are expressed as the average of duplicates.

Table 3
Membrane permeability and inhibitory activity of **10b**, **10f**, **10m** and **10n** against PTP1B and TCPTP.

Cmpd	PTP1B (μM)[a]	TCPTP (μM)[a]	P_{app} (10^{-6} cm/s)[b]
Oleanolic acid	5.8	7.3	ND
10b	0.14	2.1	2.28
10f	0.17	1.9	2.15
10m	0.07	2.3	2.41
10n	0.11	2.8	2.62
Atenolol[c]	–	–	1.77
Propranolol[c]	–	–	18.42

[a] IC_{50} values are means of triplicates.
[b] Values of parallel artificial membrane permeation assay (PAMPA)
[c] Controls in PAMPA. Atenolol represents medium membrane permeability, and propranolol represents high membrane permeability.

order to determine this effect with newly found PTP1B inhibitors, we evaluated compound **10m** on 2-NBDG uptake in HepG2 cells. As shown in Fig. 5, insulin-stimulated glucose uptake was increased for HepG2 cells treated with Pioglitazone, which was used as the positive control, and the increases were 43.6%, 52.8%, and 64.1% at 5, 10 and 20 μM, respectively. When treated with the compound **10m,** the glucose uptake in HepG2 cells was also significantly enhanced in a dose-dependent manner, slightly better than the positive control. The increased percentages were 51.0%, 66.8% and 70.5% at 5, 10 and 20 μM, respectively.

3. Conclusions

In summary, a series of novel 2-ethoxy-4-(methoxymethyl)benzamide and 2-ethoxy-5-(methoxymethyl)benzamide derivatives designed by the “bioisosteric principle” were systematically investigated as

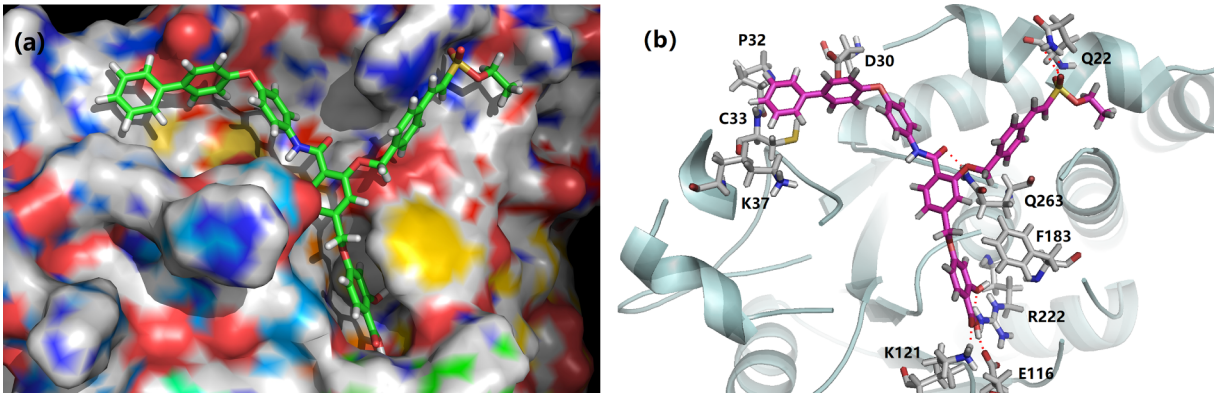

Fig. 3. Docking simulation of compound **10m** with PTP1B (PDB code 2CNE). All figures were prepared by GOLD 5.1 and PyMol. (a) Overlay of compound **10m** in the PTP1B active site. (b) Interactions of compound **10m** with PTP1B.

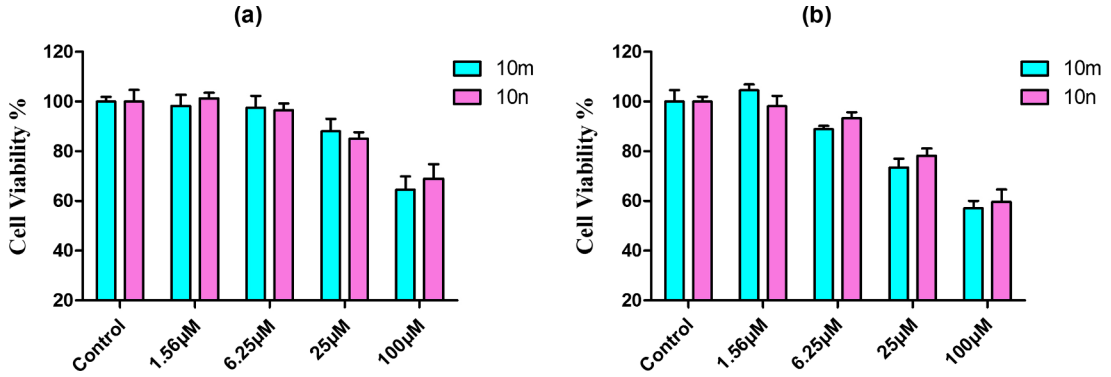

Fig. 4. Inhibitory effects of compound **10m** and **10n** on cell viability. (a) Inhibitory effects via tested compounds on HepG2 cells viability (b) Inhibitory effect via tested compounds on HL-7702 cell viability. Cells were treated with 0, 1.56, 6.25, 25 and 100 μM of tested compounds for 48 h. Each value was presented as mean ± SD, n = 3.

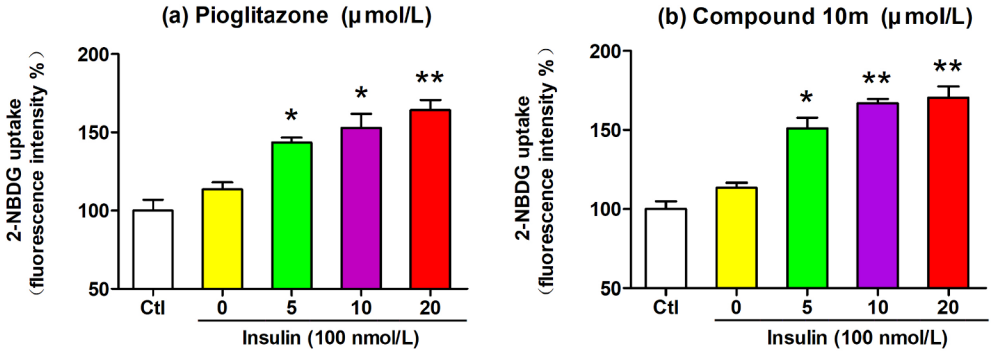

Fig. 5. Effect of compound **10m** on insulin-stimulated glucose uptake. (a) Effect of Pioglitazone on insulin-stimulated glucose uptake. (b) Effect of compound **10m** on insulin-stimulated glucose uptake. HepG2 cells were serum starved for 24 h and then incubated with various concentrations of Pioglitazone or compound **10m** (0, 5, 10 and 20 μM). After 4 h, insulin (100 nM) stimulated glucose uptake was evaluated using 2-NBDG as described in methods [34]. Each value was presented as mean ± SD, n = 3; (*) $P < 0.05$ and (**) $P < 0.01$ vs the insulin-treated group.

potentially potent and selective PTP1B inhibitors. These compounds were shown to be competitive PTP1B inhibitors. As compound **10m** showcased the most potent PTP1B activity (IC_{50} = 0.07 μM), it provided significantly improved PTP1B inhibitory activity (2 folds) and selectivity (4 folds over TCPTP) compared with the lead compound **III**. The PAMPA test indicated that these compounds have sufficient membrane permeability. Molecular docking calculated the binding mode and explained reasons for high inhibitory activity and significant selectivity of the 2-ethoxy-4-(methoxymethyl)benzamide derivatives. In addition, further studies on cell viability and cellular activity revealed that compound **10m** could enhance insulin-stimulated glucose uptake without significant cytotoxicity. These novel compounds reported could provide us a possible opportunity for the discovery of new PTP1B inhibitors with high potency, significant selectivity as well as good membrane permeability for future research.

4. Experimental section

4.1. Chemistry

4.1.1. General synthetic methods

All chemicals and solvents were obtained from commercial sources and purified using standard methods according to the need. And the solvents used were redistilled and dried by standard procedures whenever required.

Melting points were recorded on the RY-1G apparatus and are uncorrected. All reactions were monitored by thin-layer chromatography (TLC) on silica gel plates. In addition, column chromatography was performed on silica gel 300–400 mesh. ^{1}H NMR (400 MHz) and ^{13}C NMR (100 MHz) were recorded on an Agilent 400 MHz. The spin multiplicities were indicated by the symbols: s (singlet), d (doublet), t (triplet), q (quartet), m (multiplet) and brs (broad singlet). The chemical shifts were given in δ (ppm), which refer to the signal of $CDCl_3$ (δ 7.26, ^{1}H NMR and δ 77.00, ^{13}C NMR) and the signal of $(CD_3)_2SO$ (δ 2.54, ^{1}H NMR and δ 39.52, ^{13}C NMR). The chemical shift values were given in parts per million wherein coupling constants (*J*) in Hertz. High resolution mass spectroscopy was conducted using Agilent 6230 LC-MS.

4.1.2. tert-butyl 4-(bromomethyl)-2-hydroxybenzoate (2)

To a solution of 2-hydroxy-4-methylbenzoic acid (**1**) (10.0 g, 66 mmol) in 30 mL dry DMF at 0 °C, N,'N-carbonyldiimidazole (11.7 g, 72 mmol) was added, and stirred at room temperature for 1 h. Then DBU (15 mL, 100 mmol) and tert-butanol (13 mL, 130 mmol) were added in sequence, and stirred at room temperature for 5 h. The resulting mixture was diluted with H_2O and then extracted with EtOAc. The combined organic layers were washed with brine and dried over anhydrous Na_2SO_4. The solvent was removed to afford the crude product. It was purified by flash chromatography to afford tert-butyl 2-hydroxy-4-methylbenzoate as light yellow oil (12.6 g, 91%).

A mixture of tert-butyl 2-hydroxy-4-methylbenzoate (10.0 g, 48 mmol), NBS (9.3 g, 52 mmol) and AIBN (0.5 g, 3 mmol) in 100 mL CCl_4 was heated to reflux for 4 h. The resulting mixture was cooled to room temperature, filtered over celite and the organic layer was washed with saturated aqueous $NaHCO_3$, water and brine in sequence, dried over anhydrous Na_2SO_4, evaporated in vacuum and purified by flash chromatography to afford **2** as light yellow solid (5.9 g, 43%). M.p.: 44–46 °C. ^{1}H NMR (400 MHz, $CDCl_3$): *δ* 1.59 (s, 9H), 4.38 (s, 2H), 6.85 (d, *J* = 8.0 Hz, 1H), 6.95 (s, 1H), 7.73 (d, *J* = 8.0 Hz, 1H), 11.06 (s, 1H); ^{13}C NMR (100 MHz, $CDCl_3$): *δ* 28.1, 32.1, 82.9, 113.5, 117.7, 119.4, 130.5, 144.8, 161.6, 169.2; HRMS (ESI) *m/z* calcd for $C_{12}H_{15}BrO_3$ $[M+Na]^+$ 309.0097, found 309.0103.

4.1.3. tert-butyl 4-((4-formylphenoxy)methyl)-2-hydroxybenzoate (3)

A mixture of tert-butyl 4-(bromomethyl)-2-hydroxybenzoate (**2**) (2.9 g, 10 mmol), *p*-hydroxybenzaldehyde (1.4 g, 11 mmol) and K_2CO_3 (2.1 g, 15 mmol) in 50 mL MeCN was heat to reflux for 8 h. The resulting mixture was cooled to room temperature, evaporated in vacuum, and the residue was diluted with H_2O and then extracted with

EtOAc. The combined organic layers were washed with brine and dried over anhydrous Na_2SO_4. The solvent was removed to afford the crude product. It was purified by flash chromatography to afford **3** as white solid (2.6 g, 77%). M.p.: 92–94 °C. ^{1}H NMR (400 MHz, $CDCl_3$): δ 1.60 (s, 9H), 5.11 (s, 2H), 6.85 (d, J = 8.0 Hz, 1H), 7.00–7.04 (m, 3H), 7.77–7.81 (m, 3H), 9.86 (s, 1H), 11.09 (s, 1H); ^{13}C NMR (100 MHz, $CDCl_3$): δ 28.1, 69.2, 83.0, 113.4, 115.1, 115.5, 117.0, 130.2, 130.5, 131.9, 143.7, 161.9, 163.2, 169.4, 190.6; HRMS (ESI) *m/z* calcd for $C_{19}H_{20}O_5$ $[M+Na]^+$ 351.1203, found 351.1212.

4.1.4. tert-butyl 4-(((2,2-dimethyl-4-oxo-4H-benzo[d][1,3]dioxin-7-yl) oxy)methyl)-2-hydroxybenzoate ***(7)***

According to the procedure described for **3**, **2** was treated with 7-hydroxy-2,2-dimethyl-4H-benzo[d][1,3]dioxin-4-one to afford **7** (3.1 g, 80%) as white solid. M.p.: 194–196 °C. ^{1}H NMR (400 MHz, $CDCl_3$): δ 1.60 (s, 9H), 1.70 (s, 6H), 5.08 (s, 2H), 6.44 (s, 1H), 6.68 (d, J = 8.4 Hz, 1H), 6.86 (d, J = 8.4 Hz, 1H), 6.98 (s, 1H), 7.78 (d, J = 8.0 Hz, 1H), 7.85 (d, J = 8.0 Hz, 1H), 11.09 (s, 1H); ^{13}C NMR (100 MHz, $CDCl_3$): δ 25.7, 28.1, 69.3, 83.0, 102.0, 106.3, 106.6, 110.6, 113.5, 115.5, 117.0, 130.6, 131.2, 143.4, 157.8, 160.8, 161.9, 164.9, 169.4; HRMS (ESI) *m/z* calcd for $C_{22}H_{24}O_7$ $[M+H]^+$ 401.1594, found 401.1607.

4.1.5. tert-butyl (E)-2-((2,2-dimethyl-4-oxo-4H-benzo[d][1,3]dioxin-7-yl) methoxy)-4-((4-(2-(ethoxysulfonyl)vinyl)phenoxy)methyl)benzoate ***(4)***

A mixture of tert-butyl 4-((4-formylphenoxy)methyl)-2-hydroxybenzoate (**3**) (2.3 g, 7 mmol), 7-(bromomethyl)-2,2-dimethyl-4H-benzo[d][1,3]dioxin-4-one (2.2 g, 8 mmol) and K_2CO_3 (1.4 g, 10 mmol) in 50 mL MeCN was heated to reflux for 8 h. The resulting mixture was cooled to room temperature, evaporated in vacuum, then residue was diluted with H_2O and extracted with EtOAc. The combined organic layers were washed with brine and dried over anhydrous Na_2SO_4. The solvent was removed to afford the crude product. It was purified by flash chromatography to afford tert-butyl 2-((2,2-dimethyl-4-oxo-4H-benzo[d][1,3]dioxin-7-yl)methoxy)-4-((4-formylphenoxy)methyl) benzoate as white solid (2.7 g, 75%).

To a solution of tert-butyl 2-((2,2-dimethyl-4-oxo-4H-benzo[d][1,3] dioxin-7-yl)methoxy)-4-((4-formylphenoxy)methyl)benzoate (2.3 g, 4 mmol) and ethyl (diethoxyphosphoryl) methanesulfonate (1.4 g, 5 mmol) in 60 mL dry THF, NaH (60% in mineral oil) (0.3 g, 8 mmol) was added in small portions at 0 °C. Then reaction was stirred at room temperature for 4 h. The resulting mixture was quenched with saturated aqueous NH_4Cl, and extracted with EtOAc. The combined organic layers were washed with brine, dried over anhydrous Na_2SO_4, concentrated under vacuum, and purified by flash chromatography to afford **4** as white solid (2.6 g, 93%). M.p.: 152–154 °C. ^{1}H NMR (400 MHz, $CDCl_3$): δ 1.36 (t, J = 7.2 Hz, 3H), 1.55 (s, 9H), 1.70 (s, 6H), 4.19 (q, J = 7.2 Hz, 2H), 5.09 (s, 2H), 5.14 (s, 2H), 6.58 (d, J = 15.6 Hz, 1H), 6.92–7.03 (m, 4H), 7.13 (s, 1H), 7.18 (d, J = 8.0 Hz, 1H), 7.41 (d, J = 8.0 Hz, 2H), 7.49 (d, J = 15.6 Hz, 1H), 7.72 (d, J = 8.0 Hz, 1H), 7.92 (d, J = 8.0 Hz, 1H); ^{13}C NMR (100 MHz, $CDCl_3$): δ 14.8, 25.7, 28.1, 66.6, 69.2, 69.5, 81.4, 106.4, 111.9, 112.7, 115.2, 115.3, 115.4, 118.6, 119.3, 120.7, 122.7, 125.0, 129.7, 130.2, 131.6, 141.3, 144.0, 146.1, 156.1, 157.2, 160.7, 165.3; HRMS (ESI) *m/z* calcd for $C_{33}H_{36}O_{10}S$ $[M+Na]^+$ 647.1921, found 647.1931.

4.1.6. tert-butyl (E)-4-(((2,2-dimethyl-4-oxo-4H-benzo[d][1,3]dioxin-7-yl)oxy)methyl)-2-((4-(2-(ethoxysulfonyl)vinyl)benzyl)oxy)benzoate ***(8)***

According to the procedure described for **4**, **7** was treated with 4-(bromomethyl)benzaldehyde and ethyl (diethoxyphosphoryl) methanesulfonate to afford **8** (3.3 g, 69% for two steps) as white solid. M.p.: 112–114 °C. ^{1}H NMR (400 MHz, $CDCl_3$): δ 1.38 (t, J = 7.2 Hz, 3H), 1.53 (s, 9H), 1.69 (s, 6H), 4.21 (q, J = 7.2 Hz, 2H), 5.07 (s, 2H), 5.16 (s, 2H), 6.43 (s, 1H), 6.66–6.67 (m, 1H), 6.75 (d, J = 15.6 Hz, 1H), 7.00–7.01 (m, 2H), 7.49–7.85 (m, 7H); ^{13}C NMR (100 MHz, $CDCl_3$): δ 14.8, 25.7, 28.1, 66.8, 69.6, 69.8, 81.3, 102.0, 106.3, 106.6, 110.6, 111.9, 119.2, 121.3, 122.9, 127.6, 128.6, 131.2, 131.4, 131.6, 140.2, 140.6, 144.0, 157.5, 157.8, 160.7, 164.9, 165.3; HRMS (ESI) *m/z* calcd for $C_{33}H_{36}O_{10}S$ $[M+Na]^+$ 647.1921, found 647.1936.

4.1.7. (E)-2-((2,2-dimethyl-4-oxo-4H-benzo[d][1,3]dioxin-7-yl) methoxy)-4-((4-(2-(ethoxysulfonyl)vinyl)phenoxy)methyl)benzoic acid ***(5)***

To a solution of tert-butyl (E)-2-((2,2-dimethyl-4-oxo-4H-benzo[d] [1,3]dioxin-7-yl)methoxy)-4-((4-(2-(ethoxysulfonyl)vinyl)phenoxy)methyl)benzoate **(4)** (1.9 g, 3 mmol) in 3 mL dry DCM, TFA (3.4 g, 30 mmol) was added dropwise. Then the reaction was stirred at room temperature for 1 h. The resulting mixture was diluted with H_2O, and evaporated most of DCM in vacuum. The resulted precipitate was filtered and purified by flash chromatography to afford **5** as white solid (1.5 g, 84%). M.p.: 158–160 °C. ^{1}H NMR (400 MHz, DMSO-d_6): δ 1.32 (t, J = 7.2 Hz, 3H), 1.73 (s, 6H), 4.20 (q, J = 7.2 Hz, 2H), 5.25 (s, 2H), 5.34 (s, 2H), 7.10–7.16 (m, 3H), 7.29–7.35 (m, 4H), 7.58 (d, J = 15.6 Hz, 1H), 7.77–7.79 (m, 3H), 7.91 (d, J = 8.0 Hz, 1H); ^{13}C NMR (100 MHz, DMSO-d_6): δ 14.7, 25.3, 66.8, 68.6, 68.8, 106.4, 112.0, 112.7, 114.9, 115.3, 119.4, 119.6, 120.9, 121.0, 125.1, 129.2, 130.9, 131.2, 142.1, 143.7, 147.1, 155.6, 156.9, 160.0, 160.5, 166.9; HRMS (ESI) *m/z* calcd for $C_{29}H_{28}O_{10}S$ $[M+Na]^+$ 591.1295, found 591.1294.

4.1.8. (E)-4-(((2,2-dimethyl-4-oxo-4H-benzo[d][1,3]dioxin-7-yl)oxy) methyl)-2-((4-(2-(ethoxysulfonyl)vinyl)benzyl)oxy)benzoic acid ***(9)***

According to the procedure described for **5**, **8** was treated with TFA to afford **9** (1.8 g, 86%) as white solid. M.p.: 154–156 °C. ^{1}H NMR (400 MHz, $CDCl_3$): δ 1.39 (t, J = 7.2 Hz, 3H), 1.70 (s, 6H), 4.23 (q, J = 7.2 Hz, 2H), 5.13 (s, 2H), 5.31 (s, 2H), 6.46 (s, 1H), 6.68–6.70 (m, 1H), 6.75 (d, J = 15.6 Hz, 1H), 7.15–7.17 (m, 2H), 7.52–8.15 (m, 7H); ^{13}C NMR (100 MHz, $CDCl_3$): δ 14.8, 25.7, 67.0, 69.2, 71.0, 102.0, 106.4, 106.8, 110.5, 111.5, 118.1, 120.4, 122.1, 122.1, 128.2, 129.0, 131.3, 132.4, 134.0, 138.1, 143.4, 157.7, 157.8, 160.7, 164.6, 166.1; HRMS (ESI) *m/z* calcd for $C_{29}H_{28}O_{10}S$ $[M+Na]^+$ 591.1295, found 591.1311.

4.1.9. tert-butyl 5-(((tert-butyldimethylsilyl)oxy)methyl)-2-hydroxybenzoate ***(12)***

To a solution of tert-butyl 5-formyl-2-hydroxybenzoate (**11**) (6.6 g, 30 mmol) in 50 mL MeOH, $NaBH_4$ (0.6 g, 15 mmol) was added in small portions at 0 °C. Then reaction was stirred at room temperature for 1 h. The resulting mixture was quenched with saturated aqueous NH_4Cl, and extracted with EtOAc. The combined organic layers were washed with brine and dried over anhydrous Na_2SO_4. The solvent was removed to afford the crude product.

To a solution of the crude product and imidazole (2.9 g, 42 mmol) in 30 mL DMF, TBSCl (4.9 g, 32 mmol) was added in small portions at 0 °C. The reaction was stirred at room temperature overnight. Then the resulting mixture was diluted with H_2O, and extracted with EtOAc. The combined organic layers were washed with brine and dried over anhydrous Na_2SO_4. The solvent was removed to afford the yellow oil. It was purified by flash chromatography to afford the product as colorless oil (8.5 g, 83% for two steps). ^{1}H NMR (400 MHz, $CDCl_3$): δ 0.11 (s, 6H), 0.96 (s, 9H), 1.61 (s, 9H), 4.67 (s, 2H), 6.92 (d, J = 8.4 Hz, 1H), 7.35 (d, J = 8.4 Hz, 1H), 7.77 (s, 1H), 10.96 (s, 1H); ^{13}C NMR (100 MHz, $CDCl_3$): δ −5.2, 18.3, 25.9, 28.1, 64.1, 82.6, 113.3, 117.3, 127.5, 131.8, 133.0, 160.8, 169.8; HRMS (ESI) *m/z* calcd for $C_{18}H_{30}O_4Si$ $[M+Na]^+$ 361.1806, found 361.1805.

4.1.10. tert-butyl 2-((2,2-dimethyl-4-oxo-4H-benzo[d][1,3]dioxin-7-yl) methoxy)-5-(hydroxymethyl)benzoate ***(13)***

A mixture of tert-butyl 5-(((tert-butyldimethylsilyl)oxy)methyl)-2-hydroxybenzoate (**12**) (6.8 g, 20 mmol), 7-(bromomethyl)-2,2-dimethyl-4H-benzo[d][1,3]dioxin-4-one (6.6 g, 24 mmol) and K_2CO_3 (4.2 g, 30 mmol) in 100 mL MeCN was heat to reflux for 8 h. The resulting mixture was cooled to room temperature, evaporated in vacuum, and the residue was diluted with H_2O and then extracted with EtOAc. The combined organic layers were washed with brine and dried

over anhydrous Na_2SO_4. The solvent was removed to afford the crude product. It was purified by flash chromatography to afford tert-butyl 5-(((tert-butyldimethylsilyl)oxy)methyl)-2-((2,2-dimethyl-4-oxo-4H-benzo[d][1,3]dioxin-7-yl)methoxy)benzoate as white solid (7.9 g, 74%).

To a solution of tert-butyl 5-(((tert-butyldimethylsilyl)oxy)methyl)-2-((2,2-dimethyl-4-oxo-4H-benzo[d][1,3]dioxin-7-yl)methoxy) benzoate (7.5 g, 12 mmol) in 60 mL THF, TBAF (12 mL, 1 N in THF) was added dropwise at 0 °C. The reaction was stirred at room temperature for 1 h. Then the resulting mixture was diluted with H_2O, and extracted with EtOAc. The combined organic layers were washed with brine and dried over anhydrous Na_2SO_4. The solvent was removed to afford the crude product. It was purified by flash chromatography to afford the product as white solid (5.2 g, 93%). M.p.: 120–122 °C.^{1}H NMR (400 MHz, $CDCl_3$): δ 1.56 (s, 9H), 1.72 (s, 6H), 1.98 (brs, 1H), 4.63 (s, 2H), 5.15 (s, 2H), 6.91 (d, J = 8.4 Hz, 1H), 7.14 (s, 1H), 7.20 (d, J = 8.0 Hz, 1H), 7.40 (d, J = 8.4 Hz, 1H), 7.69 (s, 1H), 7.94 (d, J = 8.0 Hz, 1H); ^{13}C NMR (100 MHz, $CDCl_3$): δ 25.8, 28.2, 64.4, 69.7, 81.5, 106.4, 112.8, 113.7, 115.2, 120.7, 123.2, 129.8, 130.1, 131.4, 132.8, 133.6, 146.4, 156.3, 156.4, 165.6; HRMS (ESI) *m/z* calcd for $C_{23}H_{26}O_7$ $[M+Na]^+$ 437.1571, found 437.1583.

4.1.11. tert-butyl 2-((4-formylbenzyl)oxy)-5-(hydroxymethyl)benzoate ***(17)***

According to the procedure described for **13**, **12** was treated with 4-(bromomethyl)benzaldehyde and TBAF to afford **17** (4.1 g, 65% for two steps) as white solid. M.p.: 90–92 °C. ^{1}H NMR (400 MHz, $CDCl_3$): δ 1.53 (s, 9H), 2.74 (brs, 1H), 4.57 (s, 2H), 5.16 (s, 2H), 6.87 (d, J = 8.0 Hz, 1H), 7.34 (d, J = 8.0 Hz, 1H), 7.61–7.86 (m, 5H), 9.96 (s, 1H); ^{13}C NMR (100 MHz, $CDCl_3$): δ 28.1, 64.1, 69.8, 81.4, 113.5, 122.9, 127.2, 129.8, 129.9, 131.3, 133.5, 135.7, 143.7, 156.3, 165.7, 191.9; HRMS (ESI) *m/z* calcd for $C_{20}H_{22}O_5$ $[M+Na]^+$ 365.1359, found 365.1367.

4.1.12. tert-butyl (E)-2-((2,2-dimethyl-4-oxo-4H-benzo[d][1,3]dioxin-7-yl)methoxy)-5-((4-(2-(ethoxysulfonyl)vinyl)phenoxy)methyl)benzoate ***(14)***

To a solution of tert-butyl 2-((2,2-dimethyl-4-oxo-4H-benzo[d][1,3] dioxin-7-yl)methoxy)-5-(hydroxymethyl)benzoate (**13**) (4.2 g, 10 mmol), *p*-hydroxybenzaldehyde (1.5 g, 11 mmol) and PPh_3 (3.1 g, 12 mmol) in 30 mL dry THF, DEAD (2.1 g, 12 mmol) was added dropwise. The reaction mixture was stirred in room temperature for 12 h. After completion, the resulting mixture was evaporated in vacuum, and the residue was purified by flash chromatography to afford tert-butyl 2-((2,2-dimethyl-4-oxo-4H-benzo[d][1,3]dioxin-7-yl)methoxy)-5-((4-formylphenoxy)methyl)benzoate as white solid (2.4 g, 46%).

To a solution of tert-butyl 2-((2,2-dimethyl-4-oxo-4H-benzo[d][1,3] dioxin-7-yl)methoxy)-5-((4-formylphenoxy)methyl)benzoate (2.3 g, 4 mmol) and ethyl (diethoxyphosphoryl) methanesulfonate (1.4 g, 5 mmol) in 60 mL dry THF, NaH (60% in mineral oil) (0.3 g, 8 mmol) was added in small portions at 0 °C. Then the reaction was stirred at room temperature for 4 h. The resulting mixture was quenched with saturated aqueous NH_4Cl, and extracted with EtOAc. The combined organic layers were washed with brine, dried over anhydrous Na_2SO_4, concentrated under vacuum, and purified by flash chromatography to afford **14** as white solid (2.5 g, 89%). M.p.: 160–162 °C. ^{1}H NMR (400 MHz, $CDCl_3$): δ 1.36 (t, J = 7.2 Hz, 3H), 1.55 (s, 9H), 1.71 (s, 6H), 4.18 (q, J = 7.2 Hz, 2H), 5.02 (s, 2H), 5.15 (s, 2H), 6.58 (d, J = 15.2 Hz, 1H), 6.94–7.20 (m, 5H), 7.43–7.53 (m, 4H), 7.76 (s, 1H), 7.94 (d, J = 8.0 Hz, 1H); ^{13}C NMR (100 MHz, $CDCl_3$): δ 14.8, 25.7, 28.1, 66.5, 69.2, 69.5, 81.6, 106.4, 112.7, 113.6, 115.2, 115.3, 118.4, 120.6, 123.3, 124.8, 128.6, 129.7, 130.2, 130.7, 131.9, 144.2, 146.1, 156.2, 156.8, 160.8, 161.1, 165.4; HRMS (ESI) *m/z* calcd for $C_{33}H_{36}O_{10}S$ $[M+Na]^+$ 647.1921, found 647.1924.

4.1.13. tert-butyl (E)-5-(((2,2-dimethyl-4-oxo-4H-benzo[d][1,3]dioxin-7-yl)oxy)methyl)-2-((4-(2-(ethoxysulfonyl)vinyl)benzyl)oxy)benzoate ***(18)***

According to the procedure described for **14**, **17** was treated with 7-hydroxy-2,2-dimethyl-4H-benzo[d][1,3]dioxin-4-one and ethyl (diethoxyphosphoryl) methanesulfonate to afford **18** (2.1 g, 39% for two steps) as white solid. M.p.: 116–118 °C. ^{1}H NMR (400 MHz, $CDCl_3$): δ 1.39 (t, J = 7.2 Hz, 3H), 1.55 (s, 9H), 1.70 (s, 6H), 4.23 (q, J = 7.2 Hz, 2H), 5.01 (s, 2H), 5.19 (s, 2H), 6.48 (s, 1H), 6.68–6.70 (m, 1H), 6.75 (d, J = 15.6 Hz, 1H), 6.96–6.98 (m, 1H), 7.42–7.86 (m, 8H); ^{13}C NMR (100 MHz, $CDCl_3$): δ 14.8, 25.7, 28.1, 66.8, 69.6, 69.9, 81.5, 101.9, 106.3, 106.4, 110.7, 113.7, 121.3, 123.3, 127.6, 127.9, 128.6, 130.8, 131.2, 131.5, 132.0, 140.2, 144.0, 157.2, 157.8, 160.8, 165.1, 165.3; HRMS (ESI) *m/z* calcd for $C_{33}H_{36}O_{10}S$ $[M+Na]^+$ 647.1921, found 647.1929.

4.1.14. (E)-2-((2,2-dimethyl-4-oxo-4H-benzo[d][1,3]dioxin-7-yl) methoxy)-5-((4-(2-(ethoxysulfonyl)vinyl)phenoxy)methyl)benzoic acid ***(15)***

According to the procedure described for **5**, **14** was treated with TFA to afford **15** (1.5 g, 91%) as white solid. M.p.: 164–166 °C.^{1}H NMR (400 MHz, DMSO-d_6): δ 1.32 (t, J = 7.2 Hz, 3H), 1.73 (s, 6H), 4.19 (q, J = 7.2 Hz, 2H), 5.18 (s, 2H), 5.34 (s, 2H), 7.12 (d, J = 8.4 Hz, 2H), 7.23–7.34 (m, 4H), 7.58 (d, J = 15.6 Hz, 1H), 7.63–7.65 (m, 1H), 7.78–7.93 (m, 4H); ^{13}C NMR (100 MHz, DMSO-d_6): δ 14.7, 25.3, 66.8, 68.9, 68.6, 106.5, 112.1, 113.9, 114.9, 115.3, 119.3, 120.9, 121.5, 124.9, 128.8, 129.3, 130.8, 130.9, 132.9, 143.9, 147.2, 155.7, 156.5, 160.1, 160.7, 167.0; HRMS (ESI) *m/z* calcd for $C_{29}H_{28}O_{10}S$ $[M+Na]^+$ 591.1295, found 591.1306.

4.1.15. (E)-5-(((2,2-dimethyl-4-oxo-4H-benzo[d][1,3]dioxin-7-yl)oxy) methyl)-2-((4-(2-(ethoxysulfonyl)vinyl)benzyl)oxy)benzoic acid ***(19)***

According to the procedure described for **5**, **18** was treated with TFA to afford **19** (1.3 g, 88%) as white solid. M.p.: 128–130 °C. ^{1}H NMR (400 MHz, $CDCl_3$): δ 1.39 (t, J = 7.2 Hz, 3H), 1.70 (s, 6H), 4.22 (q, J = 7.2 Hz, 2H), 5.05 (s, 2H), 5.33 (s, 2H), 6.43 (s, 1H), 6.67–6.69 (m, 1H), 6.76 (d, J = 15.6 Hz, 1H), 7.11–7.13 (m, 1H), 7.54–7.86 (m, 7H), 8.20 (s, 1H); ^{13}C NMR (100 MHz, $CDCl_3$): δ 14.9, 25.7, 67.0, 69.2, 71.3, 102.0, 106.4, 106.7, 110.7, 113.7, 118.5, 122.3, 128.3, 129.1, 129.9, 131.3, 132.6, 133.0, 134.1, 137.9, 143.4, 157.2, 157.8, 160.8, 164.9, 165.7; HRMS (ESI) *m/z* calcd for $C_{29}H_{28}O_{10}S$ $[M+Na]^+$ 591.1295, found 591.1307.

4.1.16. General procedure for ***6a-c, 10a-p, 16a-c and 20a-c****:*

To a solution of benzoic acid derivatives (**5** or **9** or **15** or **19**, 1.0 equiv.) and HATU (1.1 equiv.) in DMF at room temperature, substituted amine (1.05 equiv.) and DIPEA (1.2 equiv.) were added sequentially. The reaction mixture was stirred at room temperature for 1–2 h. The resulting mixture was diluted with 5% HCl, and extracted with EtOAc. The combined organic layers were washed with saturated aqueous $NaHCO_3$ and brine, dried over anhydrous Na_2SO_4, concentrated, and recrystallized from MeOH to afford the crude product.

A mixture of the crude product (25–45 mg, 1.0 equiv.), HCl (12 N, 0.5 mL) and 4 mL 1,4-dioxane was stirred at room temperature for 48–96 h. The resulting mixture was diluted with H_2O and then extracted with EtOAc. The combined organic layers were washed with brine, dried over anhydrous Na_2SO_4, concentrated under vacuum, and purified by flash chromatography (DCM:MOH = 25:1) to afford the target product.

4.1.16.1. (E)-4-((5-((4-(2-(ethoxysulfonyl)vinyl)phenoxy)methyl)-2-(phenylcarbamoyl)phenoxy)methyl)-2-hydroxybenzoic acid ***(6a)***. White solid (24 mg, 66%). M.p.: 172–174 °C. ^{1}H NMR (400 MHz, DMSO-d_6): δ 1.33 (t, J = 7.2 Hz, 3H), 4.21 (q, J = 7.2 Hz, 2H), 5.28 (s, 2H), 5.31 (s, 2H), 7.09–7.22 (m, 6H), 7.29–7.38 (m, 4H), 7.58 (d, J = 15.6 Hz, 1H), 7.68–7.80 (m, 6H), 10.22 (s, 1H); ^{13}C NMR (100 MHz, DMSO-d_6): δ 14.7, 66.7, 68.8, 69.3, 112.3, 115.0, 115.3, 115.6, 117.9, 119.4,

119.9, 123.4, 125.0, 128.3, 128.6, 129.7, 130.0, 130.3, 130.8, 138.9, 140.8, 143.6, 144.7, 155.4, 160.5, 161.1, 164.1, 171.6; HRMS (ESI) *m/z* calcd for $C_{32}H_{29}NO_9S$ $[M+H]^+$ 604.1635, found 604.1638.

4.1.16.2. (E)-4-((2-((4-(4-(tert-butyl)phenoxy)phenyl)carbamoyl)-5-((4-(2-(ethoxysulfonyl)vinyl)phenoxy)methyl)phenoxy)methyl)-2-hydroxybenzoic acid ***(6b)***. White solid (26 mg, 71%). M.p.: 100–102 °C. ^{1}H NMR (400 MHz, DMSO-d_6): δ 1.31–1.34 (m, 12H), 4.21 (q, J = 7.2 Hz, 2H), 5.28 (s, 2H), 5.31 (s, 2H), 6.93–7.22 (m, 9H), 7.29–7.42 (m, 4H), 7.58 (d, J = 15.6 Hz, 1H), 7.68–7.79 (m, 6H), 10.26 (s, 1H), 11.33 (brs, 1H); ^{13}C NMR (100 MHz, DMSO-d_6): δ 14.7, 31.2, 33.9, 66.7, 68.8, 69.1, 112.2, 112.3, 115.3, 115.4, 117.3, 117.8, 119.2, 119.4, 120.0, 121.0, 125.0, 125.2, 126.5, 129.8, 130.3, 130.8, 134.7, 140.7, 143.7, 144.8, 145.2, 152.1, 155.0, 155.3, 160.5, 161.2, 164.0, 171.6; HRMS (ESI) *m/z* calcd for $C_{42}H_{41}NO_{10}S$ $[M+Na]^+$ 774.2343, found 774.2364.

4.1.16.3. (E)-4-((2-((4-dodecylphenyl)carbamoyl)-5-((4-(2-(ethoxysulfonyl)vinyl)phenoxy)methyl)phenoxy)methyl)-2-hydroxybenzoic acid ***(6c)***. Light yellow solid (13 mg, 34%). M.p.: 128–130 °C. ^{1}H NMR (400 MHz, DMSO-d_6): δ 0.88 (t, J = 6.8 Hz, 3H), 1.27–1.31 (m, 21H), 1.57–1.58 (m, 2H), 2.53–2.55 (m, 2H), 4.21 (q, J = 7.2 Hz, 2H), 5.28 (s, 2H), 5.31 (s, 2H), 7.08–7.22 (m, 7H), 7.32 (d, J = 15.6 Hz, 1H), 7.37 (s, 1H), 7.56–7.80 (m, 7H), 10.12 (s, 1H); ^{13}C NMR (100 MHz, DMSO-d_6): δ 13.8, 14.7, 22.0, 28.5, 28.6, 28.8, 28.9, 28.9, 29.0, 29.0, 31.0, 31.2, 34.5, 66.7, 68.8, 69.3, 112.2, 112.4, 115.3, 115.6, 117.8, 119.3, 119.4, 119.9, 125.0, 125.0, 128.3, 130.0, 130.3, 130.8, 136.5, 137.4, 140.8, 143.6, 144.6, 155.4, 160.5, 161.2, 163.8, 171.6; HRMS (ESI) *m/z* calcd for $C_{44}H_{53}NO_9S$ $[M+Na]^+$ 794.3333, 794.3331.

4.1.16.4. (E)-4-((3-((4-(2-(ethoxysulfonyl)vinyl)benzyl)oxy)-4-(phenylcarbamoyl)benzyl)oxy)-2-hydroxybenzoic acid ***(10a)***. White solid (19 mg, 65%). M.p.: 164–166 °C. ^{1}H NMR (400 MHz, $CDCl_3$): δ 1.33 (t, J = 7.2 Hz, 3H), 4.23 (q, J = 7.2 Hz, 2H), 5.27 (s, 2H), 5.35 (s, 2H), 6.62–6.64 (m, 2H), 7.10 (t, J = 6.8 Hz, 1H), 7.20–7.22 (m, 1H), 7.34 (t, J = 6.8 Hz, 2H), 7.41 (s, 1H), 7.52 (d, J = 15.6 Hz, 1H), 7.60–7.84 (m, 9H), 10.22 (s, 1H), 11.56 (brs, 1H); ^{13}C NMR (100 MHz, $CDCl_3$): δ 14.7, 67.2, 69.0, 69.6, 101.7, 106.0, 107.8, 112.3, 119.3, 120.0, 122.3, 123.4, 125.0, 128.2, 128.8, 129.2, 130.0, 131.7, 131.8, 139.0, 139.8, 140.8, 143.6, 155.6, 163.3, 163.9, 164.1, 171.8; HRMS (ESI) *m/z* calcd for $C_{32}H_{29}NO_9S$ $[M+H]^+$ 604.1635, found 604.1646.

4.1.16.5. (E)-4-((4-((4-(4-(tert-butyl)phenoxy)phenyl)carbamoyl)-3-((4-(2-(ethoxysulfonyl)vinyl)benzyl)oxy)benzyl)oxy)-2-hydroxybenzoic acid ***(10b)***. White solid (21 mg, 57%). M.p.: 122–124 °C. ^{1}H NMR (400 MHz, $CDCl_3$): δ 1.29–1.32 (m, 12H), 4.21 (q, J = 7.2 Hz, 2H), 5.26 (s, 2H), 5.34 (s, 2H), 6.62–6.64 (m, 2H), 6.93 (d, J = 8.4 Hz, 2H), 7.02 (d, J = 8.4 Hz, 2H), 7.19–7.21 (m, 1H), 7.39–7.42 (m, 3H), 7.50 (d, J = 15.6 Hz, 1H), 7.62–7.71 (m, 6H), 7.75–7.77 (m, 1H), 7.82–7.84 (m, 2H), 10.22 (s, 1H), 11.58 (brs, 1H); ^{13}C NMR (100 MHz, $CDCl_3$): δ 14.6, 31.2, 33.9, 67.1, 68.9, 69.5, 101.7, 105.9, 107.7, 112.3, 117.3, 119.1, 119.9, 121.0, 122.3, 125.1, 126.5, 128.1, 129.0, 129.9, 131.6, 131.8, 134.6, 139.8, 140.6, 143.5, 145.3, 152.2, 154.9, 155.4, 163.2, 163.8, 163.9, 171.7; HRMS (ESI) *m/z* calcd for $C_{42}H_{41}NO_{10}S$ $[M+Na]^+$ 774.2343, found 774.2358.

4.1.16.6. (E)-4-((4-((4-dodecylphenyl)carbamoyl)-3-((4-(2-(ethoxysulfonyl)vinyl)benzyl)oxy)benzyl)oxy)-2-hydroxybenzoic acid ***(10c)***. Yellow solid (8 mg, 31%). M.p.: 160–162 °C. ^{1}H NMR (400 MHz, $CDCl_3$): δ 0.88 (t, J = 6.8 Hz, 3H), 1.26–1.34 (m, 21H), 1.55–1.57 (m, 2H), 2.51–2.57 (m, 2H), 4.23 (q, J = 7.2 Hz, 2H), 5.26 (s, 2H), 5.34 (s, 2H), 6.62–6.64 (m, 2H), 7.13 (d, J = 8.0 Hz, 2H), 7.19 (d, J = 7.2 Hz, 1H), 7.40–7.44 (m, 1H), 7.48–7.53 (m, 3H), 7.62–7.66 (m, 3H), 7.72–7.77 (m, 2H), 7.81–7.83 (m, 2H), 10.11 (s, 1H), 11.53 (brs, 1H); ^{13}C NMR (100 MHz, $CDCl_3$): δ 14.0, 14.6, 22.0, 28.5, 28.6, 28.8, 28.8, 28.9, 30.9, 31.2, 34.5, 67.0, 68.9, 69.6, 101.7, 105.9, 107.7, 112.3, 117.3, 119.3, 119.9, 122.3, 124.8, 128.2, 128.2, 129.0, 130.0, 131.6, 131.9, 136.5, 139.7, 140.7, 143.4, 155.5, 163.2, 163.7, 163.9, 171.7; HRMS (ESI) *m/z* calcd for $C_{44}H_{53}NO_9S$ $[M+Na]^+$ 794.3333, 794.3338.

4.1.16.7. (E)-4-((3-((4-(2-(ethoxysulfonyl)vinyl)benzyl)oxy)-4-((4-phenoxyphenyl)carbamoyl)benzyl)oxy)-2-hydroxybenzoic acid ***(10d)***. White solid (25 mg, 63%). M.p.: 154–156 °C. ^{1}H NMR (400 MHz, $CDCl_3$): δ 1.30 (t, J = 7.2 Hz, 3H), 4.21 (q, J = 7.2 Hz, 2H), 5.27 (s, 2H), 5.35 (s, 2H), 6.62–6.64 (m, 2H), 6.99–7.06 (m, 4H), 7.14 (t, J = 6.8 Hz, 1H), 7.19–7.22 (m, 1H), 7.38–7.41 (m, 4H), 7.51 (d, J = 15.2 Hz, 1H), 7.64–7.85 (m, 8H), 10.26 (s, 1H), 11.56 (brs, 1H); ^{13}C NMR (100 MHz, $CDCl_3$): δ 14.7, 67.2, 69.0, 69.6, 101.8, 106.0, 107.8, 112.4, 117.9, 119.5, 119.9, 120.0, 121.1, 122.4, 123.0, 125.1, 128.2, 129.1, 130.0, 131.7, 131.9, 135.0, 139.9, 140.7, 143.6, 151.9, 155.6, 157.4, 163.3, 163.9, 164.1, 171.8; HRMS (ESI) *m/z* calcd for $C_{38}H_{33}NO_{10}S$ $[M+Na]^+$ 718.1717, found 718.1733.

4.1.16.8. (E)-4-((3-((4-(2-(ethoxysulfonyl)vinyl)benzyl)oxy)-4-((4-(4-ethylphenoxy)phenyl)carbamoyl)benzyl)oxy)-2-hydroxybenzoic acid ***(10e)***. White solid (17 mg, 55%). M.p.: 172–174 °C. ^{1}H NMR (400 MHz, $CDCl_3$): δ 1.20 (t, J = 7.2 Hz, 3H), 1.31 (t, J = 7.2 Hz, 3H), 2.61 (q, J = 7.2 Hz, 2H), 4.21 (q, J = 7.2 Hz, 2H), 5.26 (s, 2H), 5.34 (s, 2H), 6.62–6.64 (m, 2H), 6.92 (d, J = 8.4 Hz, 2H), 7.00 (d, J = 8.4 Hz, 2H), 7.19–7.24 (m, 3H), 7.40 (s, 1H), 7.50 (d, J = 15.6 Hz, 1H), 7.62–7.71 (m, 6H), 7.75–7.77 (m, 1H), 7.82–7.84 (m, 2H), 10.22 (s, 1H), 11.55 (brs, 1H); ^{13}C NMR (100 MHz, $CDCl_3$): δ 14.7, 15.7, 27.4, 67.2, 69.0, 69.6, 101.8, 106.0, 107.8, 112.4, 118.0, 119.2, 120.0, 121.1, 122.4, 125.2, 126.6, 128.2, 129.1, 130.0, 131.7, 131.9, 134.7, 138.5, 139.9, 140.7, 143.6, 152.4, 155.2, 155.5, 163.3, 163.9, 164.0, 171.7; HRMS (ESI) *m/z* calcd for $C_{40}H_{37}NO_{10}S$ $[M+Na]^+$ 746.2030, found 746.2035.

4.1.16.9. (E)-4-((3-((4-(2-(ethoxysulfonyl)vinyl)benzyl)oxy)-4-((4-(4-isopropylphenoxy)phenyl)carbamoyl)benzyl)oxy)-2-hydroxybenzoic acid ***(10f)***. White solid (20 mg, 70%). M.p.: 176–178 °C. ^{1}H NMR (400 MHz, $CDCl_3$): δ 1.23 (d, J = 6.8 Hz, 6H), 1.31 (t, J = 7.2 Hz, 3H), 2.89–2.93 (m, 1H), 4.21 (q, J = 7.2 Hz, 2H), 5.26 (s, 2H), 5.34 (s, 2H), 6.62–6.64 (m, 2H), 6.93 (d, J = 8.4 Hz, 2H), 7.01 (d, J = 8.4 Hz, 2H), 7.19–7.27 (m, 3H), 7.40 (s, 1H), 7.50 (d, J = 15.2 Hz, 1H), 7.62–7.71 (m, 6H), 7.75–7.77 (m, 1H), 7.82–7.84 (m, 2H), 10.22 (s, 1H), 11.54 (brs, 1H); ^{13}C NMR (100 MHz, $CDCl_3$): δ 14.7, 24.0, 32.7, 67.0, 69.0, 69.6, 101.8, 106.0, 107.8, 112.3, 117.8, 119.1, 120.0 121.0, 122.3, 125.2, 127.6, 128.1, 129.1, 130.0, 131.7, 131.9, 134.6, 139.8, 140.6, 143.0, 143.5, 152.3, 155.0, 155.1, 155.4, 163.3, 163.9, 171.7; HRMS (ESI) *m/z* calcd for $C_{41}H_{39}NO_{10}S$ $[M+Na]^+$ 760.2187, found 760.2205.

4.1.16.10. (E)-4-((3-((4-(2-(ethoxysulfonyl)vinyl)benzyl)oxy)-4-((4-(4-fluorophenoxy)phenyl)carbamoyl)benzyl)oxy)-2-hydroxybenzoic acid ***(10g)***. White solid (19 mg, 62%). M.p.: 174–176 °C. ^{1}H NMR (400 MHz, $CDCl_3$): δ 1.32 (t, J = 7.2 Hz, 3H), 4.21 (q, J = 7.2 Hz, 2H), 5.26 (s, 2H), 5.34 (s, 2H), 6.62–6.64 (m, 2H), 7.01–7.07 (m, 4H), 7.19–7.26 (m, 3H), 7.40 (s, 1H), 7.50 (d, J = 15.6 Hz, 1H), 7.62–7.71 (m, 6H), 7.75–7.77 (m, 1H), 7.82–7.84 (m, 2H), 10.23 (s, 1H), 11.54 (brs, 1H); ^{13}C NMR (100 MHz, $CDCl_3$): δ 14.7, 67.1, 69.0, 69.5, 101.8, 106.0, 107.7, 112.4, 116.3, 116.5, 119.0, 119.8, 119.9, 121.0, 122.3, 125.0, 128.1, 129.0, 130.0, 131.6, 131.8, 134.8, 139.8, 140.6, 143.4, 152.3 and 153.3, 155.5 and 156.7, 159.1, 163.2, 163.9, 164.0, 171.7; HRMS (ESI) *m/z* calcd for $C_{38}H_{32}FNO_{10}S$ $[M+Na]^+$ 736.1623, found 736.1633.

4.1.16.11. (E)-4-((4-((4-(4-chlorophenoxy)phenyl)carbamoyl)-3-((4-(2-C(ethoxysulfonyl)vinyl)benzyl)oxy)benzyl)oxy)-2-hydroxybenzoic acid ***(10h)***. White solid (15 mg, 48%). M.p.: 136–138 °C. ^{1}H NMR (400 MHz, $CDCl_3$): δ 1.29–1.46 (m, 3H), 3.66–4.22 (m, 2H), 5.27–5.35 (m, 4H), 6.62–6.64 (m, 2H), 6.90–6.96 (m, 2H), 7.02–7.07

(m, 4H), 7.19–7.21 (m, 1H), 7.41–7.46 (m, 3H), 7.52–7.57 (m, 3H), 7.62–7.84 (m, 6H), 10.26–10.28 (m, 1H), 11.56 (brs, 1H); ^{13}C NMR (100 MHz, $CDCl_3$): δ 14.7and 18.8, 67.1, 69.0, 70.0, 101.8, 106.0, 107.8, 112.4, 119.5, 121.1, 124.8, 126.7, 127.2, 128.1, 128.2, 129.1, 129.8, 129.9, 130.0, 131.7, 134.8, 135.1, 135.2, 136.6, 140.8, 151.5, 155.7, 156.3, 163.3, 163.9, 164.0, 171.7; HRMS (ESI) *m/z* calcd for $C_{38}H_{32}ClNO_{10}S$ $[M+Na]^+$ 752.1327, found 752.1343.

4.1.16.12. (E)-4-((4-((4-(4-bromophenoxy)phenyl)carbamoyl)-3-((4-(2-(ethoxysulfonyl)vinyl)benzyl)oxy)benzyl)oxy)-2-hydroxybenzoic acid ***(10i)***. White solid (28 mg, 74%). M.p.: 168–170 °C. ^{1}H NMR (400 MHz, $CDCl_3$): δ 1.32 (t, J = 7.2 Hz, 3H), 4.21 (q, J = 7.2 Hz, 2H), 5.26 (s, 2H), 5.35 (s, 2H), 6.62–6.64 (m, 2H), 6.97 (d, J = 8.4 Hz, 2H), 7.07 (d, J = 8.4 Hz, 2H), 7.20–7.22 (m, 1H), 7.40 (s, 1H), 7.51 (d, J = 15.6 Hz, 1H), 7.55–7.57 (m, 2H), 7.62–7.72 (m, 6H), 7.75–7.77 (m, 1H), 7.82–7.84 (m, 2H), 10.27 (s, 1H), 11.56 (brs, 1H); ^{13}C NMR (100 MHz, $CDCl_3$): δ 14.7, 67.1, 69.0, 69.6, 101.8, 106.0, 107.8, 112.4, 114.5, 119.8, 119.9, 120.0, 121.1, 122.4, 125.1, 128.2, 129.1, 130.0, 131.7, 131.9, 132.7, 135.4, 139.9, 140.7, 143.5, 151.3, 155.5, 156.9, 163.3, 163.9, 164.1, 171.8; HRMS (ESI) *m/z* calcd for $C_{38}H_{32}BrNO_{10}S$ $[M+Na]^+$ 796.0822, found 796.0826.

4.1.16.13. (E)-4-((3-((4-(2-(ethoxysulfonyl)vinyl)benzyl)oxy)-4-((4-(4-(trifluoromethoxy)phenoxy)phenyl)carbamoyl)benzyl)oxy)-2-hydroxybenzoic acid ***(10j)***. White solid (26 mg, 65%). M.p.: 170–172 °C. ^{1}H NMR (400 MHz, $CDCl_3$): δ 1.31 (t, J = 7.2 Hz, 3H), 4.21 (q, J = 7.2 Hz, 2H), 5.27 (s, 2H), 5.35 (s, 2H), 6.62–6.64 (m, 2H), 7.09–7.11 (m, 4H), 7.19–7.21 (m, 1H), 7.38–7.41 (m, 3H), 7.50 (d, J = 15.6 Hz, 1H), 7.62–7.67 (m, 3H), 7.69–7.77 (m, 4H), 7.82–7.84 (m, 2H), 10.28 (s, 1H), 11.55 (brs, 1H); ^{13}C NMR (100 MHz, $CDCl_3$): δ 14.7, 67.1, 69.0, 69.6, 101.8, 106.0, 107.8, 112.4, 118.9, 120.0, 121.1, 122.4, 122.9, 125.2, 128.1, 129.1, 129.9, 131.7, 131.9, 135.5, 139.9, 140.7, 143.2, 143.3, 143.6, 151.3, 155.5, 156.4, 163.3, 163.9, 164.1, 171.8; HRMS (ESI) *m/z* calcd for $C_{39}H_{32}F_3NO_{11}S$ $[M+Na]^+$ 802.1540, found 802.1541.

4.1.16.14. (E)-4-((3-((4-(2-(ethoxysulfonyl)vinyl)benzyl)oxy)-4-((4-(4-(trifluoromethyl)phenoxy)phenyl)carbamoyl)benzyl)oxy)-2-hydroxybenzoic acid ***(10k)***. White solid (17 mg, 56%). M.p.: 178–180 °C. ^{1}H NMR (400 MHz, $CDCl_3$): δ 1.31 (t, J = 7.2 Hz, 3H), 4.21 (q, J = 7.2 Hz, 2H), 5.27 (s, 2H), 5.35 (s, 2H), 6.62–6.64 (m, 2H), 7.15–7.22 (m, 5H), 7.41 (s, 1H), 7.50 (d, J = 15.6 Hz, 1H), 7.62–7.84 (m, 11*H*), 10.32 (s, 1H), 11.55 (brs, 1H); ^{13}C NMR (100 MHz, $CDCl_3$): δ 14.6, 67.0, 68.9, 69.6, 101.8, 105.9, 107.7, 112.3, 117.3, 119.9, 120.6, 121.1, 122.4, 125.1, 127.3, 127.4, 128.1, 129.1, 130.0, 131.7, 131.9, 136.0, 139.8, 140.7, 143.5, 150.2, 155.5, 160.9, 163.2, 163.9, 164.1, 171.7; HRMS (ESI) *m/z* calcd for $C_{39}H_{32}F_3NO_{10}S$ $[M+Na]^+$ 786.1591, found 786.1604.

4.1.16.15. (E)-4-((3-((4-(2-(ethoxysulfonyl)vinyl)benzyl)oxy)-4-((4-(4-nitrophenoxy)phenyl)carbamoyl)benzyl)oxy)-2-hydroxybenzoic acid ***(10l)***. White solid (24 mg, 61%). M.p.: 164–166 °C. ^{1}H NMR (400 MHz, $CDCl_3$): δ 1.31 (t, J = 7.2 Hz, 3H), 4.21 (q, J = 7.2 Hz, 2H), 5.26 (s, 2H), 5.35 (s, 2H), 6.62–6.64 (m, 2H), 7.13–7.21 (m, 5H), 7.42 (s, 1H), 7.50 (d, J = 15.6 Hz, 1H), 7.56–7.84 (m, 9H), 8.25–8.28 (m, 2H), 10.36 (s, 1H), 11.55 (brs, 1H); ^{13}C NMR (100 MHz, $CDCl_3$): δ 14.7, 67.1, 69.0, 69.6, 101.8, 106.0, 107.8, 112.3, 116.9, 119.9, 121.0, 121.2, 122.3, 125.1, 126.1, 127.2, 128.1, 129.1, 130.0, 131.7, 131.9, 136.5, 139.9, 140.8, 142.1, 143.5, 149.6, 155.5, 163.3, 163.9, 164.2, 171.8; HRMS (ESI) *m/z* calcd for $C_{38}H_{32}N_2O_{12}S$ $[M+Na]^+$ 763.1568, found 763.1592.

4.1.16.16. (E)-4-((4-((4-([1,1′-biphenyl]-4-yloxy)phenyl)carbamoyl)-3-((4-(2-(ethoxysulfonyl)vinyl)benzyl)oxy)benzyl)oxy)-2-hydroxybenzoic acid ***(10m)***. White solid (24 mg, 73%). M.p.: 186–188 °C. ^{1}H NMR (400 MHz, $CDCl_3$): δ 1.30 (t, J = 7.2 Hz, 3H), 4.21 (q, J = 7.2 Hz, 2H), 5.27 (s, 2H), 5.35 (s, 2H), 6.62–6.64 (m, 2H), 7.10 (t, J = 6.8 Hz, 4H), 7.20–7.22 (m, 1H), 7.38–7.41 (m, 2H), 7.47–7.55 (m, 4H), 7.64–7.85 (m, 12H), 10.28 (s, 1H), 11.59 (brs, 1H); ^{13}C NMR (100 MHz, $CDCl_3$): δ 14.7, 67.1, 69.0, 69.6, 101.8, 106.0, 107.7, 112.3, 118.1, 119.7, 120.0, 121.1, 122.3, 125.1, 126.4, 127.1, 128.1, 128.2, 128.9, 129.1, 130.0, 131.7, 131.9, 134.9, 135.1, 139.5, 139.9, 140.7, 143.5, 151.7, 155.5, 157.1, 163.3, 163.9, 164.0, 171.8; HRMS (ESI) *m/z* calcd for $C_{44}H_{37}NO_{10}S$ $[M+Na]^+$ 794.2030, found 794.2035.

4.1.16.17. (E)-4-((3-((4-(2-(ethoxysulfonyl)vinyl)benzyl)oxy)-4-((4-(naphthalen-2-yloxy)phenyl)carbamoyl)benzyl)oxy)-2-hydroxybenzoic acid ***(10n)***. White solid (28 mg, 72%). M.p.: 190–192 °C. ^{1}H NMR (400 MHz, $CDCl_3$): δ 1.30 (t, J = 7.2 Hz, 3H), 4.21 (q, J = 7.2 Hz, 2H), 5.28 (s, 2H), 5.35 (s, 2H), 6.62–6.64 (m, 2H), 7.14 (d, J = 8.4 Hz, 2H), 7.21 (d, J = 7.6 Hz, 1H), 7.31–7.36 (m, 2H), 7.41–7.56 (m, 4H), 7.63–7.78 (m, 7H), 7.83–7.85 (m, 3H), 7.92–8.00 (m, 2H), 10.30 (s, 1H), 11.56 (brs, 1H); ^{13}C NMR (100 MHz, $CDCl_3$): δ 14.7, 67.1, 69.0, 69.5, 101.7, 105.9, 107.8, 112.3, 112.5, 119.3, 119.8, 121.1, 122.3, 124.6, 125.1, 126.6, 127.0, 127.6, 128.1, 129.1, 129.5, 129.9, 130.0, 131.7, 131.9, 133.9, 135.2, 139.9, 140.7, 142.4, 143.5, 151.7, 155.3, 155.5, 163.3, 163.9, 164.1, 171.8; HRMS (ESI) *m/z* calcd for $C_{42}H_{35}NO_{10}S$ $[M+Na]^+$ 768.1874, found 768.1876.

4.1.16.18. (E)-4-((3-((4-(2-(ethoxysulfonyl)vinyl)benzyl)oxy)-4-((4-hexylphenyl)carbamoyl)benzyl)oxy)-2-hydroxybenzoic acid ***(10o)***. White solid (14 mg, 44%). M.p.: 176–178 °C. ^{1}H NMR (400 MHz, $CDCl_3$): δ 0.89 (t, J = 7.2 Hz, 3H), 1.30–1.35 (m, 9H), 1.54–1.58 (m, 2H), 2.53–2.58 (m, 2H), 4.23 (q, J = 7.2 Hz, 2H), 5.26 (s, 2H), 5.34 (s, 2H), 6.62–6.64 (m, 2H), 7.14 (d, J = 8.0 Hz, 2H), 7.20 (d, J = 7.6 Hz, 1H), 7.40 (s, 1H), 7.48–7.53 (m, 3H), 7.62–7.66 (m, 3H), 7.71–7.77 (m, 2H), 7.82–7.84 (m, 2H), 10.12 (s, 1H), 11.54 (brs, 1H); ^{13}C NMR (100 MHz, $CDCl_3$): δ 13.9, 14.6, 22.0, 28.2, 30.9, 31.0, 34.5, 67.0, 68.9, 69.6, 101.7, 105.9, 107.7, 112.3, 119.3, 119.9, 122.3, 124.9, 128.2, 128.3, 129.0, 131.6, 131.9, 136.6, 137.5, 139.8, 140.6, 142.4, 143.5, 155.5, 163.3, 163.8, 163.9, 171.7; HRMS (ESI) *m/z* calcd for $C_{38}H_{41}NO_9S$ $[M+Na]^+$ 710.2394, found 710.2393.

4.1.16.19. (E)-4-((3-((4-(2-(ethoxysulfonyl)vinyl)benzyl)oxy)-4-(hexadecylcarbamoyl)benzyl)oxy)-2-hydroxybenzoic acid ***(10p)***. White solid (9 mg, 31%). M.p.: 158–160 °C. ^{1}H NMR (400 MHz, $CDCl_3$): δ 0.87 (t, J = 6.8 Hz, 3H), 1.17–1.25 (m, 26H), 1.33 (t, J = 7.2 Hz, 3H), 1.37–1.41 (m, 2H), 3.24–3.26 (m, 2H), 4.23 (q, J = 7.2 Hz, 2H), 5.21 (s, 2H), 5.30 (s, 2H), 6.59–6.61 (m, 2H), 7.13 (d, J = 8.4 Hz, 1H), 7.34 (s, 1H), 7.50 (d, J = 15.6 Hz, 1H), 7.62–7.66 (m, 3H), 7.73 (t, J = 8.0 Hz, 2H), 7.83–7.85 (m, 2H), 8.07–8.09 (m, 1H), 11.53 (brs, 1H); ^{13}C NMR (100 MHz, $CDCl_3$): δ 13.9, 14.7, 22.0, 26.4, 28.6, 28.7, 28.8, 28.9, 29.0, 29.0, 31.3, 67.0, 69.0, 69.9, 101.7, 105.9, 107.6, 112.3, 119.8, 122.4, 123.9, 128.3, 129.1, 130.3, 131.6, 131.9, 139.7, 140.4, 143.4, 155.7, 163.3, 163.9, 164.7, 171.7; HRMS (ESI) *m/z* calcd for $C_{42}H_{57}NO_9S$ $[M+Na]^+$ 774.3646, found 774.3649.

4.1.16.20. (E)-4-((4-((4-(2-(ethoxysulfonyl)vinyl)phenoxy)methyl)-2-(phenylcarbamoyl)phenoxy)methyl)-2-hydroxybenzoic acid ***(16a)***. White solid (13 mg, 43%). M.p.: 176–178 °C. ^{1}H NMR (400 MHz, DMSO-d_6): δ 1.32 (t, J = 7.2 Hz, 3H), 4.21 (q, J = 7.2 Hz, 2H), 5.22 (s, 2H), 5.31 (s, 2H), 7.07–7.16 (m, 4H), 7.27–7.36 (m, 5H), 7.58 (d, J = 15.6 Hz, 1H), 7.60–7.63 (m, 1H), 7.69–7.71 (m, 2H), 7.78–7.80 (m, 4H), 10.26 (s, 1H), 11.34 (brs, 1H); ^{13}C NMR (100 MHz, DMSO-d_6): δ 14.7, 66.7, 68.7, 69.3, 112.3, 113.3, 115.3, 115.5, 117.8, 119.3, 119.4, 123.5, 124.8, 125.4, 128.6, 129.1, 129.5, 130.3, 130.8, 131.5, 138.9, 143.7, 144.7, 155.0, 160.7, 161.2, 164.1, 171.6; HRMS (ESI) *m/z* calcd for $C_{32}H_{29}NO_9S$ $[M+H]^+$ 604.1635, found 604.1649.

4.1.16.21. (E)-4-((2-((4-(4-(tert-butyl)phenoxy)phenyl)carbamoyl)-4-((4-(2-(ethoxysulfonyl)vinyl)phenoxy)methyl)phenoxy)methyl)-2-hydroxybenzoic acid ***(16b)***. White solid (14 mg, 43%). M.p.:

102–104 °C. ^{1}H NMR (400 MHz, DMSO-d_6): δ 1.31–1.34 (m, 12H), 4.19 (q, J = 7.2 Hz, 2H), 5.21 (s, 2H), 5.31 (s, 2H), 6.92–7.08 (m, 5H), 7.12–7.15 (m, 3H), 7.26–7.32 (m, 2H), 7.39–7.42 (m, 2H), 7.58 (d, J = 16.0 Hz, 1H), 7.60–7.62 (m, 1H), 7.71–7.79 (m, 6H), 10.29 (s, 1H), 11.38 (brs, 1H); ^{13}C NMR (100 MHz, DMSO-d_6): δ 14.7, 31.2, 34.0, 66.7, 68.7, 69.2, 112.3, 113.3, 115.3, 115.4, 117.3, 117.7, 119.2, 119.3, 121.1, 124.8, 125.7, 126.5, 129.1, 129.4, 130.3, 130.8, 131.5, 134.7, 143.7, 144.8, 145.2, 152.2, 154.9, 155.0, 160.7, 161.2, 164.0, 171.6; HRMS (ESI) *m/z* calcd for $C_{42}H_{41}NO_{10}S$ $[M+Na]^+$ 774.2343, found 774.2346.

4.1.16.22. (E)-4-((2-((4-dodecylphenyl)carbamoyl)-4-((4-(2-(ethoxysulfonyl)vinyl)phenoxy)methyl)phenoxy)methyl)-2-hydroxybenzoic acid ***(16c)***. Light yellow solid (7 mg, 28%). M.p.: 122–124 °C. ^{1}H NMR (400 MHz, DMSO-d_6): δ 0.86 (t, J = 6.8 Hz, 3H), 1.26–1.34 (m, 21H), 1.55–1.58 (m, 2H), 2.54–2.58 (m, 2H), 4.20 (q, J = 7.2 Hz, 2H), 5.21 (s, 2H), 5.31 (s, 2H), 7.07–7.16 (m, 6H), 7.26 (s, 1H), 7.30 (d, J = 15.6 Hz, 1H), 7.56–7.62 (m, 4H), 7.77–7.79 (m, 4H), 10.16 (s, 1H), 11.36 (brs, 1H); ^{13}C NMR (100 MHz, DMSO-d_6): δ 13.8, 14.6, 22.0, 28.3, 28.6, 28.8, 28.9, 29.0, 30.9, 31.2, 34.5, 66.7, 68.7, 69.3, 112.3, 113.3, 115.3, 115.5, 117.8, 119.3, 119.5, 124.8, 125.4, 128.3, 129.1, 129.5, 130.4, 130.8, 131.5, 136.5, 137.5, 143.7, 144.7, 155.0, 160.7, 161.2, 163.8, 171.6; HRMS (ESI) *m/z* calcd for $C_{44}H_{53}NO_9S$ $[M+Na]^+$ 794.3333, 794.3342.

4.1.16.23. (E)-4-((4-((4-(2-(ethoxysulfonyl)vinyl)benzyl)oxy)-3-(phenylcarbamoyl)benzyl)oxy)-2-hydroxybenzoic acid ***(20a)***. White solid (17 mg, 57%). M.p.: 160–162 °C. ^{1}H NMR (400 MHz, DMSO-d_6): δ 1.33 (t, J = 7.2 Hz, 3H), 4.23 (q, J = 7.2 Hz, 2H), 5.20 (s, 2H), 5.35 (s, 2H), 6.62 (s, 2H), 7.11 (t, J = 7.2 Hz, 1H), 7.31–7.37 (m, 3H), 7.51 (d, J = 15.6 Hz, 1H), 7.61–7.66 (m, 6H), 7.73–7.84 (m, 4H), 10.25 (s, 1H), 11.55 (brs, 1H); ^{13}C NMR (100 MHz, DMSO-d_6): δ 14.7, 67.1, 68.9, 69.7, 101.7, 105.8, 107.8, 113.5, 119.5, 122.4, 123.6, 125.5, 128.2, 128.8, 129.0, 129.1, 129.2, 129.6, 131.7, 131.9, 138.9, 139.9, 143.5, 155.2, 163.3, 164.1, 164.2, 171.8; HRMS (ESI) *m/z* calcd for $C_{32}H_{29}NO_9S$ $[M+Na]^+$ 626.1455, found 626.1468.

4.1.16.24. (E)-4-((3-((4-(4-(tert-butyl)phenoxy)phenyl)carbamoyl)-4-((4-(2-(ethoxysulfonyl)vinyl)benzyl)oxy)benzyl)oxy)-2-hydroxybenzoic acid ***(20b)***. White solid (14 mg, 43%). M.p.: 118–120 °C. ^{1}H NMR (400 MHz, DMSO-d_6): δ 1.30–1.34 (m, 12H), 4.21 (q, J = 7.2 Hz, 2H), 5.19 (s, 2H), 5.35 (s, 2H), 6.62 (s, 2H), 6.94 (d, J = 8.0 Hz, 2H), 7.02 (d, J = 8.0 Hz, 2H), 7.29–7.32 (m, 1H), 7.41 (d, J = 8.0 Hz, 2H), 7.50 (d, J = 15.2 Hz, 1H), 7.60–7.69 (m, 6H), 7.73–7.89 (m, 4H), 10.27 (s, 1H), 11.54 (brs, 1H); ^{13}C NMR (100 MHz, DMSO-d_6): δ 14.7, 31.2, 34.0, 67.0, 68.8, 69.6, 101.7, 105.7, 107.7, 113.4, 117.4, 119.1, 121.1, 122.3, 125.4, 126.5, 128.0, 129.0, 129.1, 129.5, 131.5, 131.6, 131.8, 134.6, 139.8, 143.5, 145.3, 152.2, 154.9, 155.1, 163.3, 164.0, 164.1, 171.7; HRMS (ESI) *m/z* calcd for $C_{42}H_{41}NO_{10}S$ $[M+Na]^+$ 774.2343, found 774.2347.

4.1.16.25. (E)-4-((3-((4-dodecylphenyl)carbamoyl)-4-((4-(2-(ethoxysulfonyl)vinyl)benzyl)oxy)benzyl)oxy)-2-hydroxybenzoic acid ***(20c)***. White solid (11 mg, 32%). M.p.: 184–186 °C. ^{1}H NMR (400 MHz, DMSO-d_6): δ 0.86–0.88 (m, 3H), 1.26–1.34 (m, 21H), 1.52–1.59 (m, 2H), 2.53–2.59 (m, 2H), 4.23 (q, J = 7.2 Hz, 2H), 5.19 (s, 2H), 5.35 (s, 2H), 6.61 (s, 2H), 7.13–7.15 (m, 2H), 7.30–7.32 (m, 1H), 7.48–7.66 (m, 7H), 7.73–7.76 (m, 1H), 7.78–7.84 (m, 3H), 10.16 (s, 1H), 11.55 (brs, 1H); ^{13}C NMR (100 MHz, DMSO-d_6): δ 13.9, 14.6, 22.0, 28.5, 28.6, 28.7, 28.9, 30.9, 31.2, 34.5, 67.0, 68.8, 69.6, 101.6, 105.7, 107.7, 113.4, 119.4, 122.4, 125.3, 127.1, 128.1, 128.3, 129.0, 129.5, 131.6, 131.8, 135.1, 136.5, 137.5, 139.8, 143.4, 155.1, 163.2, 163.8, 164.0, 171.7; HRMS (ESI) *m/z* calcd for $C_{44}H_{53}NO_9S$ $[M+Na]^+$ 794.3333, 794.3350.

4.2. Biological assays

4.2.1. PTP1B and TCPTP inhibition assays

The inhibitory activity of target compounds against PTP1B and TCPTP was determined with our published procedure, using *p*-nitrophenol phosphate (*p*-NPP) as the substrate [23]. Briefly, tested compounds were predisposed in 96-well micro plates as 1 μL aliquots per well in DMSO. On assay plates, the protein enzymatic assay was carried out in a total volume of 100 uL per well with 60 nM recombinant protein (PTP1B or TCPTP), 2.5 mM pNPP, 10 mM Tris, 25 mM NaCl and 1 mM EDTA (pH = 7.1). After being incubated at 37 °C for 0.5 h, the assay was terminated by an addition of 10 μL of 2 M NaOH. Then, using a microplate reader, the released *p*-nitrophenolate ion (pNP) was determined by measuring the absorbance at 405 nm. The IC_{50} values of tested compounds were shown in the Table 1, Table 2 and Table 3.

4.2.2. PTP1B kinetics assay

Unlike PTP1B enzymatic assay that used a fixed concentration of pNPP, PTP1B kinetics assay required different concentrations of pNPP. Therefore, we selected five different final concentrations of pNPP (i.e. 2 mM, 4 mM, 8 mM, 16 mM and 32 mM, respectively) with the assay buffer within this experiment. For each concentration, 50 μL of pNPP dilution was taken and added to wells of 96-well plates. Then, 1 μL of compound dilution at the concentrations of 0 μM (100% DMSO), 5 μM, 10 μM and 20 μM was added to each well that contained 50 μL of pNPP dilution, respectively. Lastly, 50 μL of PTP1B (120 nM) that had been diluted in assay buffer was added to the well so as to initiate the reaction. At the same time, the reaction mixture without the enzyme was set as a control. The plate reader recorded the FI value of the reaction mixture in each well at every two minutes and eventually calculated the enzymatic velocity of the enzymatic reaction based on the time-FI plot. The Lineweaver-Burk plot was generated by GraphPad Prism 5 in order to determine the type of PTP1B inhibition and K_i.

In the presence of the competitive inhibitor, the Michaelis-Menten equation is described as:

$$\frac{1}{v} = \frac{K_m}{V_{max} * [s]} * \left(1 + \frac{[I]}{K_i}\right) + \frac{1}{V_{max}}$$

where

v – the initial rate,
K_m – the Michaelis-Menten constant,
V_{max} – the maximum rate,
[S] – the substrate concentration,
[*I*] – the inhibitor concentration,
K_i – the inhibition constant.

The Ki value was obtained by the linear replot of **apparent K_m** from the primary reciprocal plot versus the inhibitor concentration **[*I*]** according to the equation:

$$\text{apparent}K_m = \left(1 + \frac{[I]}{K_i}\right) * K_m$$

4.2.3. Parallel artificial membrane permeability assay (PAMPA)

With our previously published method, parallel artificial membrane permeability assay was tested [24]. Briefly, 5 μL of PAMPA Lipid Blend I (Avanti 888787) was added to the filter of the donor (upper) compartment, and an artificial membrane was to be formed. Then, 150 μL of physiological saline (pH = 7.4) was added to the acceptor (lower) compartment in triplicates, and the donor compartment was placed on the acceptor compartment. Subsequently, 150 μL (5 μM final concentration, diluted with physiological saline) of tested compound was added to the donor compartment. The lid was covered, and the plate

incubated at room temperature for 18 h. The permeation of compound across an artificial membrane was quantified by LC-MS.

The apparent permeability for each compound (P_{app}) was calculated from the following equation:

$$p_{app} = \{-\ln\left(1 - \frac{[drug_{acceptor}]}{[drug_{eqilibrium}]}\right)\} * \frac{V_D * V_A}{(V_D + V_A) * area * time}$$

where

$[drug]_{acceptor}$ – the concentration of test compound in acceptor compartments,
$[drug]_{equilibrium}$ – the concentration of test compound in the total volume of the donor and acceptor compartments,
V_D – the volumes of the donor compartments,
V_A – the volumes of the acceptor compartments,
Area – surface area of the membrane multiplied by the porosity (0.31 cm^2),
Time – time of the assay,
P_{app} was expressed in 10^{-6} cm/s

4.2.4. Cell viability assay

HepG2 and HL-7702 cells were cultured in DMEM (for HepG2) or 1640 (for HL-7702) supplemented with 10% fetal bovine serum for 24 h with 5% CO_2 at 37 °C. As for cell viability assay, 5×10^3 cells were seeded in each well of 96-well plates and treated with varying concentrations of the compounds. Then, the cells were incubated in a culture medium for 48 h before an addition of 10 μL CCK-8 solution (Cell Counting Kit-8, Beyotime) to each well. Cells were incubated for another 1–2 h in the incubator at 37 °C within a dark place. Wells containing only media were used for background correction. The optical density was measured spectrophotometrically at 450 nm by a micro plate reader.

4.2.5. Effect of compound on 2-NBDG uptake by HepG2 cells

Glucose uptake in HepG2 cells was measured using 2-NBDG as previously described with minor revisions [34]. Cells were cultured in DMEM supplemented with 10% fetal bovine serum for 24 h with 5% CO_2 at 37 °C. As for the 2-NBDG uptake assay, 5×10^4 cells were seeded in each well of the 24-well plates. After treating cells with the varying concentrations of compounds for 24 h, the medium was removed, and the cells were washed twice with PBS. Then, HepG2 cells were treated with insulin (100 nM, final concentration) for 10 min, and followed by the addition of fluorescent glucose analog 2-NBDG (60 μM, final concentration) for 60 min. The uptake of 2-NBDG was measured by a FACS Calibur (BD) set at an excitation wave length of 485 nm and an emission wave length of 535 nm.

4.3. Molecular docking

The docking simulations were performed on GOLD 5.1. The default parameters were used unless otherwise stated. The 5 different structures of PTP1B (1AAX, 1G1H, 1LQF, 1Q6T and 2CNE) were loaded into GOLD, followed by superimposition into the protein structure 1AAX. Hydrogen was added, while water molecules as well ligands were deleted from the protein structure. The binding site was determined using the point 45.484, 14.573 and 5.329 at a radius of 20 Å. All possible ligand flexibility options were turned on, while early termination was turned off. Every possible form of the inhibitor molecule was docked into the protein. The generated poses were checked manually. Finally, the acceptable pose with a high score as well as a reasonable binding mode was selected and presented with Pymol 1.7.

Acknowledgments

We thank the Medicine and Engineering interdisciplinary Research Fund of Shanghai Jiao Tong University (YG2015QN03, YG2014MS10 and YG2017MS77), National Natural Science Foundation of China (81202397) and Shanghai Natural Science Fund (12ZR1415400) for the financial support.

Declaration of Competing Interest

The authors state no conflict of interest.

References

[1] J.M. Zabolotny, K.K. Bence-Hanulec, A. Stricker-Krongrad, F. Haj, Y. Wang, Y. Minokoshi, Y.B. Kim, J.K. Elmquist, L.A. Tartaglia, B.B. Kahn, B.G. Neel, PTP1B regulates leptin signal transduction in vivo, Dev. Cell 2 (2002) 489–495.
[2] H. Umemori, T. Hayashi, T. Inoue, S. Nakanishi, K. Mikoshiba, T. Yamamoto, Involvement of protein tyrosine phosphatases in activation of the trimeric G protein Gq/11, Oncogene 18 (1999) 7399.
[3] N.K. Tonks, Protein tyrosine phosphatases: from genes, to function, to disease, Nat. Rev. Mol. Cell Biol. 7 (2006) 833–846.
[4] J.C.H. Byon, A.B. Kusari, J. Kusari, Protein-tyrosine phosphatase-1B acts as a negative regulator of insulin signal transduction, Mol. Cell. Biochem. 182 (1998) 101–108.
[5] S.G. Julien, N. Dubé, S. Hardy, M.L. Tremblay, Inside the human cancer tyrosine phosphatome, Nat. Rev. Cancer 11 (2011) 35–49.
[6] K.A. Kenner, E. Anyanwu, J.M. Olefsky, J. Kusari, Protein-tyrosine phosphatase 1B is a negative regulator of insulin- and insulin-like growth factor-I-stimulated signaling, J. Biol. Chem. 271 (1996) 19810–19816.
[7] B.A. Zinker, C.M. Rondinone, J.M. Trevillyan, R.J. Gum, J.E. Clampit, J.F. Waring, N. Xie, D. Wilcox, P. Jacobson, L. Frost, P.E. Kroeger, R.M. Reilly, S. Koterski, T.J. Opgenorth, R.G. Ulrich, S. Crosby, M. Butler, S.F. Murray, R.A. McKay, S. Bhanot, B.P. Monia, M.R. Jirousek, PTP1B antisense oligonucleotide lowers PTP1B protein, normalizes blood glucose, and improves insulin sensitivity in diabetic mice, Proc. Natl. Acad. Sci. 99 (2002) 11357–11362.
[8] X.Q. Li, Q. Xu, J. Luo, L.J. Wang, B. Jiang, R.S. Zhang, D.Y. Shi, Design, synthesis and biological evaluation of uncharged catechol derivatives as selective inhibitors of PTP1B, Eur. J. Med. Chem. 136 (2017) 348–359.
[9] Y. Zhang, Y. Du, The development of protein tyrosine phosphatase1B inhibitors defined by binding sites in crystalline complexes, Future Med. Chem. 10 (2018) 2345–2367.
[10] B. Zhang, G. Salituro, D. Szalkowski, Z. Li, Y. Zhang, I. Royo, D. Vilella, M.T. Díez, F. Pelaez, C. Ruby, R.L. Kendall, X. Mao, P. Griffin, J. Calaycay, J.R. Zierath, J.V. Heck, R.G. Smith, D.E. Moller, Discovery of a small molecule insulin mimetic with antidiabetic activity in mice, Science 284 (1999) 974–977.
[11] L.D. Klaman, O. Boss, O.D. Peroni, J.K. Kim, J.L. Martino, J.M. Zabolotny, N. Moghal, M. Lubkin, Y.B. Kim, A.H. Sharpe, A. Stricker-Krongrad, G.I. Shulman, B.G. Neel, B.B. Kahn, Increased energy expenditure, decreased adiposity, and tissue-specific insulin sensitivity in protein-tyrosine phosphatase 1B-deficient mice, Mol. Cell. Biol. 20 (2000) 5479–5489.
[12] T.R. Burke, B. Ye, X. Yan, S. Wang, Z. Jia, L. Chen, Z.Y. Zhang, D. Barford, Small molecule interactions with protein−tyrosine phosphatase PTP1B and their use in inhibitor design, Biochemistry 35 (1996) 15989–15996.
[13] M.Z.S. Qian, Y. He, W. Wang, S. Liu, Recent advances in the development of protein tyrosine phosphatase 1B inhibitors for Type 2 diabetes, Future Med. Chem. 8 (2016) 1239–1258.
[14] M. Verma, S.J. Gupta, A. Chaudhary, V.K. Garg, Protein tyrosine phosphatase 1B inhibitors as antidiabetic agents – a brief review, Bioorg. Chem. 70 (2017) 267–283.
[15] S. Basu, U.V. Prasad, D.A. Barawkar, S. De, V.P. Palle, S. Menon, M. Patel, S. Thorat, U.P. Singh, K.D. Sarma, Y. Waman, S. Niranjan, V. Pathade, A. Gaur, S. Reddy, S. Ansari, Discovery of novel and potent heterocyclic carboxylic acid derivatives as protein tyrosine phosphatase 1B inhibitors, Bioorg. Med. Chem. Lett. 22 (2012) 2843–2849.
[16] L. Zhang, Y. Ge, H.M. Song, Q.M. Wang, C.H. Zhou, Design, synthesis of novel azolyl flavonoids and their protein tyrosine Phosphatase-1B inhibitory activities, Bioorg. Chem. 80 (2018) 195–203.
[17] P. Liu, Y. Du, L. Song, J. Shen, Q. Li, Novel, potent, selective and cellular active ABC type PTP1B inhibitors containing (methanesulfonyl-phenyl-amino)-acetic acid methyl ester phosphotyrosine mimetic, Bioorg. Med. Chem. 23 (2015) 7079–7088.
[18] D.P. Wilson, Z.K. Wan, W.-X. Xu, S.J. Kirincich, B.C. Follows, D. Joseph-McCarthy, K. Foreman, A. Moretto, J. Wu, M. Zhu, E. Binnun, Y.L. Zhang, M. Tam, D.V. Erbe, J. Tobin, X. Xu, L. Leung, A. Shilling, S.Y. Tam, T.S. Mansour, J. Lee, Structure-based optimization of protein tyrosine phosphatase 1B inhibitors: from the active site to the second phosphotyrosine binding site, J. Med. Chem. 50 (2007) 4681–4698.
[19] X. Li, L. Wang, D. Shi, The design strategy of selective PTP1B inhibitors over TCPTP, Bioorg. Med. Chem. 24 (2016) 3343–3352.
[20] I.G. Boutselis, X. Yu, Z.Y. Zhang, R.F. Borch, Synthesis and cell-based activity of a potent and selective protein tyrosine phosphatase 1B inhibitor prodrug, J. Med. Chem. 50 (2007) 856–864.
[21] G. Liu, Z. Xin, H. Liang, C. Abad-Zapatero, P.J. Hajduk, D.A. Janowick, B.G. Szczepankiewicz, Z. Pei, C.W. Hutchins, S.J. Ballaron, M.A. Stashko, T.H. Lubben, C.E. Berg, C.M. Rondinone, J.M. Trevillyan, M.R. Jirousek, Selective protein tyrosine phosphatase 1B inhibitors: targeting the second phosphotyrosine binding site with non-carboxylic acid-containing ligands, J. Med. Chem. 46 (2003) 3437–3440.

[22] Y. Jia, L. Lu, M. Zhu, C. Yuan, S. Xing, X. Fu, A dioxidovanadium (V) complex of NNO-donor schiff base as a selective inhibitor of protein tyrosine phosphatase 1B: synthesis, characterization, and biological activities, Eur. J. Med. Chem. 128 (2017) 287–292.

[23] J. Liu, F. Jiang, Y. Jin, Y. Zhang, J. Liu, W. Liu, L. Fu, Design, synthesis, and evaluation of 2-substituted ethenesulfonic acid ester derivatives as protein tyrosine phosphatase 1B inhibitors, Eur. J. Med. Chem. 57 (2012) 10–20.

[24] F. Yang, F. Xie, Y. Zhang, Y. Xia, W. Liu, F. Jiang, C. Lam, Y. Qiao, D. Xie, J. Li, L. Fu, Y-shaped bis-arylethenesulfonic acid esters: potential potent and membrane permeable protein tyrosine phosphatase 1B inhibitors, Bioorg. Med. Chem. Lett. 27 (2017) 2166–2170.

[25] P.J. Ala, L. Gonneville, M. Hillman, M. Becker-Pasha, E.W. Yue, B. Douty, B. Wayland, P. Polam, M.L. Crawley, E. McLaughlin, R.B. Sparks, B. Glass, A. Takvorian, A.P. Combs, T.C. Burn, G.F. Hollis, R. Wynn, Structural insights into the design of nonpeptidic isothiazolidinone-containing inhibitors of protein-tyrosine phosphatase 1B, J. Biol. Chem. 281 (2006) 38013–38021.

[26] N. Maheshwari, C. Karthikeyan, S.V. Bhadada, C. Sahi, A.K. Verma, N.S. Hari Narayana Moorthy, P. Trivedi, Synthesis and biological evaluation of some N-(3-(1H-tetrazol-5-yl) phenyl)acetamide derivatives as novel non-carboxylic PTP1B inhibitors designed through bioisosteric modulation, Bioorgan. Chem. 80 (2018) 145–150.

[27] X. Zhang, Y. He, S. Liu, Z. Yu, Z.X. Jiang, Z. Yang, Y. Dong, S.C. Nabinger, L. Wu, A.M. Gunawan, L. Wang, R.J. Chan, Z.Y. Zhang, Salicylic acid based small molecule inhibitor for the oncogenic Src homology-2 domain containing protein tyrosine phosphatase-2 (SHP2), J. Med. Chem. 53 (2010) 2482–2493.

[28] B.D.G. Page, S. Fletcher, P. Yue, Z. Li, X. Zhang, S. Sharmeen, A. Datti, J.L. Wrana, S. Trudel, A.D. Schimmer, J. Turkson, P.T. Gunning, Identification of a non-phosphorylated, cell permeable, small molecule ligand for the Stat3 SH2 domain, Bioorg. Med. Chem. Lett. 21 (2011) 5605–5609.

[29] S. Haftchenary, A.O. Jouk, I. Aubry, A.M. Lewis, M. Landry, D.P. Ball, A.E. Shouksmith, C.V. Collins, M.L. Tremblay, P.T. Gunning, Identification of bidentate salicylic acid inhibitors of PTP1B, ACS Med. Chem. Lett. 6 (2015) 982–986.

[30] S. Fletcher, J. Singh, X. Zhang, P. Yue, B.D.G. Page, S. Sharmeen, V.M. Shahani, W. Zhao, A.D. Schimmer, J. Turkson, P.T. Gunning, Disruption of transcriptionally active stat3 dimers with non-phosphorylated, salicylic acid-based small molecules: potent in vitro and tumor cell activities, ChemBioChem 10 (2009) 1959–1964.

[31] K.F. Liew, K.L. Chan, C.Y. Lee, Blood–brain barrier permeable anticholinesterase aurones: synthesis, structure–activity relationship, and drug-like properties, Eur. J. Med. Chem. 94 (2015) 195–210.

[32] F. Wohnsland, B. Faller, High-throughput permeability pH profile and high-throughput alkane/water log P with artificial membranes, J. Med. Chem. 44 (2001) 923–930.

[33] A. Maeda, K. Kai, M. Ishii, T. Ishii, M. Akagawa, Safranal, a novel protein tyrosine phosphatase 1B inhibitor, activates insulin signaling in C2C12 myotubes and improves glucose tolerance in diabetic KK-Ay mice, Mol. Nutr. Food Res. 58 (2014) 1177–1189.

[34] F. Xie, F. Yang, Y. Liang, L. Li, Y. Xia, F. Jiang, W. Liu, Y. Qi, S.R. Chowdhury, D. Xie, L. Fu, Investigation of stereoisomeric bisarylethenesulfonic acid esters for discovering potent and selective PTP1B inhibitors, Eur. J. Med. Chem. 164 (2019) 408–422.